imposed magnetic field was accommodated through a corresponding body force term in eq. (8.45). In this manner the influence of the magnetic field on the performance of the tundish was evaluated.

REFERENCES

1. Currie, I.G. (1974). *Fundamental Mechanics of Fluids*. McGraw-Hill Book Co., N.Y.
2. Timoshenko, S. and Goodier, J.W. (1951). *Theory of Elasticity*. McGraw-Hill Book Co., N.Y., 2nd ed.
3. Reddy, J.N. and Rasmussen, M.L. (1982). *Advanced Engineering Analysis*, John Wiley & Sons, N.Y.
4. Sokolnikoff, I.S. (1956). *Mathematical Theory of Elasticity*. Tata McGraw-Hill, Bombay, 2nd ed.
5. Potter, M.C. and Foss, J.F. (1975). *Fluid Mechanics*. Ronald Press, New York, p. 185.
6. Gallagher, R.H. et al. (eds.) (1975). *Finite Elements in Fluids*. John Wiley & Sons, N.Y., vol. 1.
7. Baker, A.J. (1985). *Finite Element Computational Fluid Mechanics*. McGraw-Hill Book Co., N.Y., p. 270.
8. Zienkiewicz, O.C., Liu, Y.C. and Huang, G.C. (1988). Error estimation and adaptivity in flow formulation for forming problems. *Int. J. Num. Meth. Engg.*, 25: 23-42.
9. Thomas, J.R., Hughes, W.K., Liu, Y.C, and Brooks, A. (1979). Finite element analysis of incompressible viscous flows by the penalty function formulation *J. Computational Physics*, 30: 1-60.
10. Lee, C.H. and Kobayashi, S. (1973) New solutions to rigid-plastic deformation problems using a matrix method. *Trans. ASME J. Engg. Ind.*, pp. 865-873.
11. Kobayashi, S., Oh, S.I. and Altan, T. (1989). *Metal Forming and the Finite Element Method*. Oxford Univ. Press, pp. 83-86.
12. Gresho, P.M. and Sani, R.L. (1988). On pressure boundary conditions for the incompressible Navier-Stokes equations. In: *Finite Elements in Fluids*, vol. 7 (R.H. Gallagher et al., eds.). John Wiley & Sons, N.Y., pp. 123-157.
13. Shiau, Y.C. and Kobayashi, S. (1988). Three-dimensional finite element analysis of open-die forging *Int. J. Num. Meth. Engg.*, 25: 67-85.
14. Connar and Brebbia, (1976). *Finite Element Technique for Fluid Flow*. Newnes-Butterworths, London, pp. 145-147.
15. Aoyagi, Y., Takenaka, Y., Niino, S., Watanabe, A. and Joka, I. (1988). Numerical simulation and experimental observation of coolant flow around cylinder liners in V-8 engine. *SAE Trans, J. Engines*, pp. 6.141-6.151.
16. Ilegbusi, O.J. and Szekely, J. (1989). Effect of externally imposed magnetic field on tundish performance. *Ironmaking and Steelmaking*, 16 (2): 110-115.

Chapter 9

MATERIAL NON-LINEARITY INCLUDING PLASTICITY

9.1 INTRODUCTION

Non-linearity in material properties generally signifies a variation in these properties within the useful range of application. Some properties, such as thermal conductivity, specific heat or viscosity change with temperature. Metals and alloys possess a distinct yield point above which the slope of stress-strain curve changes drastically. All these non-linearities should be considered in finite element analysis if it is desired to obtain results with sufficient accuracy. For convenience in understanding and analysis, material non-linearity may be classified into two categories:

1) Reversible non-linearity
2) Irreversible non-linearity

Thermally induced non-linearities, such as variation in thermal conductivity, specific heat or even the latent heat absorption or release during melting or solidification are reversible in nature. A decrease in temperature may bring the properties back to the original level. In contrast, material plasticity is an irreversible property and once an object is strained plastically the removal of load does not bring the object back to its original state and plastic strain remains in it. Even the yield point undergoes a permanent change. These two types of non-linearities require different analysis strategies.

9.2 REVERSIBLE NON-LINEARITY

Consideration of reversible non-linearity is fairly straightforward. Analysis steady-state heat transfer by conduction can be taken for illustration. The matrix equation governing the finite element analysis for this case is given as

$$[H]\ \{T\} - \{f\}^{(1)} = 0 \qquad \ldots (9.1)$$

[1]The derivation of this equation for temperature dependent (or coordinate dependent) thermal conductivity should now be based on weighted residue formulation on the more exact form of the heat conduction equation given by

$$\frac{\partial}{\partial x}\left(k_x \frac{\partial T}{\partial x}\right) + \frac{\partial}{\partial y}\left(k_y \frac{\partial T}{\partial y}\right) + \frac{\partial}{\partial z}\left(k_z \frac{\partial T}{\partial z}\right) + \dot{Q} = 0$$

Material properties, such as thermal conductivity appear in the terms of matrix $[H]$. For constant properties, $[H]$ does not depend on temperature and temperature vector $\{T\}$ can be determined by direct inversion of eq. (9.1). When thermal conductivity depends on temperature the terms of matrix $[H]$ cannot be determined correctly without a knowledge of actual temperature distribution. Use of a non-linear expression to represent thermal conductivity as a function of temperature will not help directly because the form of matrix $[H]$ will now become so complex that obtaining the solution becomes impossible. The procedure commonly used for solution of such problems is to start from some assumed value of the property and then apply iterative correction successively until the near exact solution is obtained. Two strategies adopted for this purpose are direct iteration technique and use of Newton-Raphson method.

9.2.1 Direct Iteration

This is a simple but effective approach to tackle reversible non-linearity. The first trial solution is obtained by taking thermal conductivity value at an initially assumed temperature (or temperature distribution). Matrix $[H]$ is determined explicitly using this value and direct inversion of eq. (9.1) gives the first trial value of the temperature vector $\{T\}$ (say $\{T^1\}$). The approximate temperature at different nodes now being known, the value of property (thermal conductivity here) is recalculated in different elements based on the nature of its variation with temperature. Use of these new values gives the modified matrix $[H]$, (say $[H^1]$), which is again used in eq. (9.1) to obtain the second modified value of the temperature vector $\{T^2\}$. This gives the basis for the next modification of thermal conductivity and consequently new matrix $[H]$, (say $[H^2]$), is obtained. Subsequent substitution into eq. (9.1) and its inversion gives the third approximation of the temperature vector $\{T^3\}$. The procedure is continued until the desired solution is obtained. Some convergence criterion is fixed and the iterations are terminated when this criterion is met. A common convergence criterion considers the difference between temperature in current iteration and previous iteration. This difference is represented as ε_i for the i-th node and the largest absolute value of ε_i at any node is compared with the preset criterion (say ε); when $|\varepsilon_i|_{\max} \leq \varepsilon$, the iteration is terminated. Often, the absolute value of ε_i is replaced by its square $(\varepsilon_i)^2_{\max}$ or its ratio with nodal temperature, $|\varepsilon_i/T_i|_{\max}$ or $(\varepsilon_i/T_i)^2_{\max}$. Using ratio or fractional error has the advantage of allowing the same percentage error at every node. It also has the disadvantage of giving undue importance to nodes where the temperature change is unimportant. For example, if we are interested in obtaining the temperature rise in a cutting tool during turning operation, we know that maximum heating will take place at the tool tip where the temperature

may reach 600–700°C while at points far away from the tip the temperature may rise by only a few degrees above room temperature (say a temperature of 40°C). An error of 4°C at these points away from the tip may represent a high percentage error of 10% while a variation of 50°C at the tool tip may indicate only 8.3% error, which is smaller in absolute terms. However, significance of the error at the tool tip is more and error criterion of permitting an absolute variation of temperature of 10°C anywhere on the tool may serve the purpose better. The more logical consideration would be the temperature variation at points where the temperature is rising rapidly and choice of absolute temperature change would be a more appropriate criterion. Several other definitions of the convergence criterion are also used. This simple approach called direct iteration, though effective, may result in lack of convergence, especially if a high degree of non-linearity exists. The relaxation factor is sometimes used to improve convergence. The Newton-Raphson method also improves convergence. Before discussing these techniques in detail, let us examine the direct iteration technique further.

Explanation of basis of direct iteration technique: For simplicity we consider eq. (9.1) for one component vector $\{T\}$ for which matrix $[H]$ will also be a single term coefficient. Representing variable $\{T\}$ by x and $[H]$ by m, eq. (9.1) can be rewritten as

$$mx - c = 0 \qquad \ldots (9.2)$$

If m is constant eq. (9.2) gives the value of x directly. When m is a complicated function of x this becomes a non-linear expression. Although direct solution of this equation may still be possible, we shall use this example to illustrate the application of direct iteration technique for determining the value of x. To use this technique we make an initial guess of the value of x at which we determine m and solve (9.2) to obtain the second value of x and then proceed with subsequent iterations. Thus we encounter a number of values of x which are not the solution of this equation implying that the right side of eq. (9.2) is non zero for all these values of x. We represent the right side by y knowing that the solution is obtained when $y = 0$. The relation between x and y is a non-linear relation given as

$$y = mx - c \qquad \ldots (9.3)$$

This relation is represented pictorially in Fig. 9.1. The solution of the equation is $x = x_f$ for which $y = 0$. If the initial guess is taken as m_0, eq. (9.3) represents a straight line which passes through a point $x = 0$, $y = -c$ and which has a slope m_0. This line is represented as (1) in Fig. (9.1) and its equation is

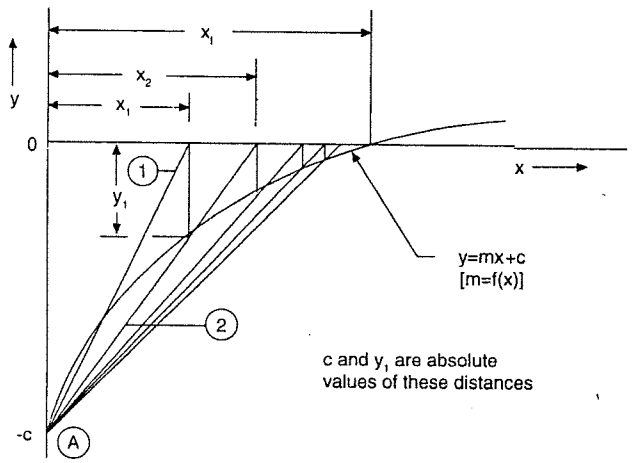

Fig. 9.1 Representation of direct iteration method.

$$y = m_0 x - c \qquad \ldots (9.4)$$

Referring back to our explanation of the direct iteration procedure, the first iterated value of x is obtained on substituting $m = m_0$ in eq. (9.2) and thus

$$x_1 = \frac{c}{m_0} \qquad \ldots (9.5)$$

This is also the value of x along line (1) for a point along x-axis ($y = 0$). Referring to Fig. 9.1, the exact value of y for $x = x_1$ is $-y_1$. Thus on substitution into eq. (9.3), we get

$$-y_1 = m_1 x_1 - c \qquad \ldots (9.6)$$

where m_1 is the value of m corresponding to $x = x_1$ or $m_1 = (c - y_1)/x_1$. This can also be visualized as the slope of a line $y = m_1 x - c$ which passes through points $x_1, -y_1$ and $0, -c$. This line is shown as line (2) in Fig. 9.1. Referring back to our direct iteration procedure once again, the second iterated value of x is obtained by substituting $m = m_1$ in eq. (9.2), i.e.

$$x_2 = \frac{c}{m_1} \qquad \ldots (9.7)$$

This is also obtained by substituting $y = 0$ into the equation of line (2) [i.e. $y = m_1 x - c$]. The value is shown as x_2 in Fig. 9.1. This procedure can be repeated for subsequent iterations. In the geometrical sense this procedure can be explained by the following description.

Using assumed value for m ($= m_0$) draw a line passing through point A and having slope m_0. Intersection of this line with x-axis gives the first guess for x (say x_1). Draw vertical line $x = x_1$ and obtain the point of its intersection with the curve representing relation between y and x. Join this point of intersection with (A) and extend the line up to x axis. The intercept gives the second iterated value of x ($= x_2$). Repeat this procedure for subsequent steps until the final value of x (i.e., x_f) is approached.

The shortcomings of this procedure are that improvement in the values of x slows down with successive iterations as we approach close to final value. Thus number of iterations turn out to be very large. Secondly, the iterated values sometimes oscillate about the exact value or these start moving away from it (divergence). Fig. 9.2 shows such situations.

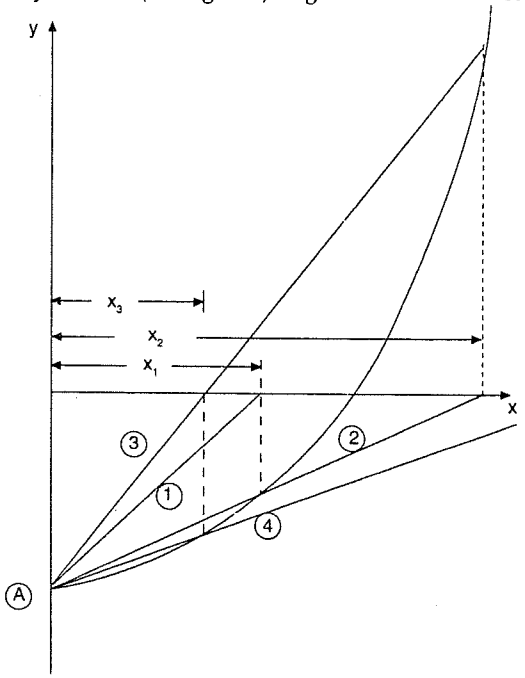

Fig. 9.2 Oscillation and divergence during direct iteration process.

9.2.2 Improving Convergence through Use of Relaxation Factor

Divergence observed under conditions shown in Fig. 9.2 can be controlled and convergence obtained by using the relaxation factor. The logic behind

use of the relaxation factor is that if we have a situation wherein the value after n-th iteration is smaller than the correct value (say $x_n < x_f$) and the value obtained after n +1-th iteration becomes larger that x_f (i.e. solution oscillates), then choosing the modified value of x_{n+1} somewhere in-between x_n and calculated x_{n+1} (say x'_{n+1}) will always result in reduced error. Thus

$$(x_{n+1})_{\text{mod}} = x_n + (x'_{n+1} - x_n) \cdot R \quad \text{(where } R < 1\text{)} \qquad \ldots (9.8)$$

The factor R is called the relaxation factor. Use of this factor is shown in Fig. 9.3 for the same case for which divergence occurred in Fig. 9.2. Now $x'_2, x'_3 \ldots x'_{n+1}$ are the new values as calculated by using the direct iteration method from the previous value of x; x_2, x_3 ... x_{n+1} are the values selected by use of the relaxation factor (0.8 in Fig. 9.3). It is obvious from the Figure that convergence has been obtained.

Under the situation shown in Fig. 9.1 for which solution is obtained after a large number of iterations, the relaxation factor greater than 1 can be used with advantage for reducing the total number of iterations.

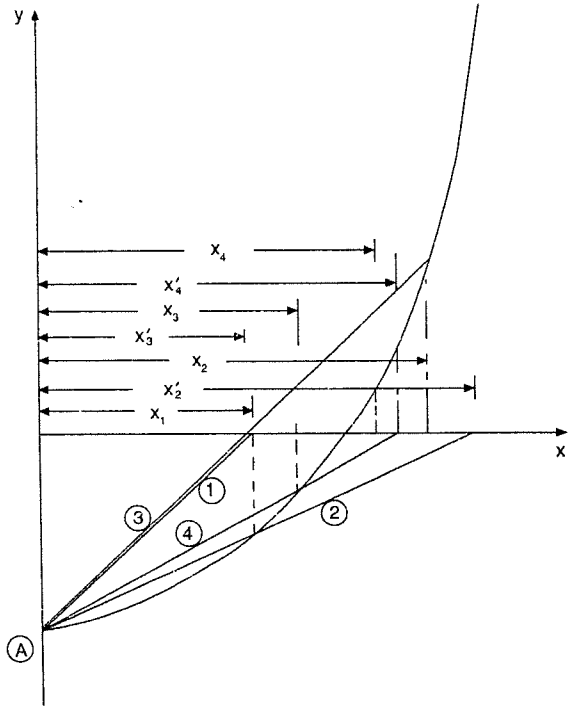

Fig. 9.3 Improved convergence by use of relaxation factor.

9.2.3 Newton-Raphson Method

We first illustrate the method with the example of a single variable as in the previous section. The relation between error term y (say y_n for n-th iteration) and parameter x is given by eq. (9.3). Representing m as m (x), being a function of x, we write

$$y = m\,(x) \cdot x - c, \qquad \ldots (9.9)$$

where m (x) is a function of x. If we know the value of y after n-th iteration (say y_n) and our interest is in an adjacent value of y (say y_{n+1}), which may be taken as the value after n+1-th iteration for convenience, we can expand eq. (9.9) using the Taylor series expansion. Thus

$$y_{n+1} = y_n + \left|\frac{dy}{dx}\right|_{\text{at } x=x_n} \cdot \Delta x + \text{higher order terms} \qquad \ldots (9.10)$$

Representing dy/dx at $x = x_n$ by k_n and Δx by Δx_n for this n-th iteration we obtain, after neglecting higher order terms,

$$y_{n+1} = y_n + K_n \cdot \Delta x_n \qquad \ldots (9.11)$$

We now shift temporarily to the graphic representation of the situation as presented in Fig. 9.4. This is similar to the case shown in Fig. 9.1. After obtaining the first iterated value of x (say x_1) using an initial guess of m_0, we proceed as follows.

At a point on the curve which corresponds to $x = x_1$, we draw a tangent, the slope of which will be $dy/dx\,|_{\text{at } x = x1}$ (or K_1). The equation of this tangent which has slope K_1 and which passes through the point $x = x_1$, $y = y_1$ can be written as

$$y - y_1 = K_1\,(x - x_1) \qquad \ldots (9.12)$$

The intercept which this line makes with x-axis (say x_2) is given by

$$K_1\,(x_2 - x_1) = -\,y_1$$

or,
$$x_2 - x_1 = -\,\frac{1}{K_1} \cdot y_1 \qquad \ldots (9.13)$$

If this increment in x is represented as Δx_1 we obtain the following relationship,

$$\Delta x_1 = -\,\frac{1}{K_1} \cdot y_1 \qquad \ldots (9.14)$$

We can now establish the guidelines for another method of iterative correction of the value of x.

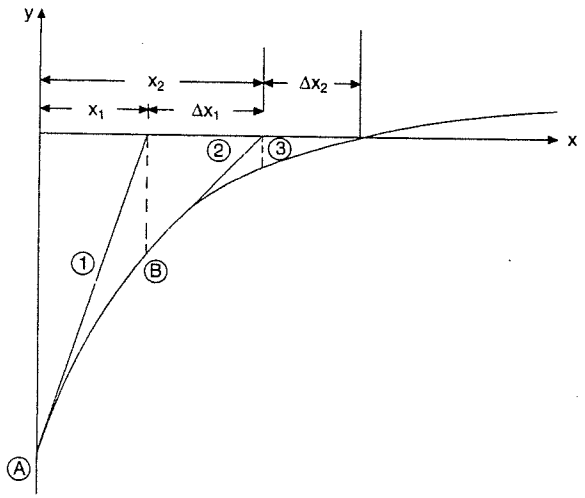

Fig. 9.4 Newton Raphson method.

First determine initial value of x (say x_1) using assumed value of m_0. Find slope of curve at point $x = x_1$ and call it K_1. The increment (correction) in the value of x is given by eq. (9.14). Use the new value of x ($x_2 = x_1 + \Delta x_1$) and proceed for another iterative correction. This approach is called the Newton-Raphson approach and it makes use of the slope of the curve (K) for subsequent iterations. Two points emerge from the discussion of this approach. First, convergence is faster, as shown in Fig. 9.4. Second, even when we approach the final value of x, the magnitude of iterative correction is appreciable, which again means only a few iterations. This approach also results in convergence even in those cases in which the direct iteration method does not converge (see Figs. 9.2 and 9.5).

9.2.4 Newton-Raphson Method for Multivariable Case

We shall now extend the Newton-Raphson procedure to the matrix equation encountered in finite element analysis. The variable is now a multicomponent vector and its coefficient is a matrix, the terms of which depend on magnitude of the vector. In thermal analysis the equation is given as

$$[H]\{T\} - \{f\} = 0$$

The order of matrix $[H]$ is $m \times m$ and that of vectors $\{T\}$ and $\{f\}$ is $m \times 1$. This matrix equation actually comprises a set of m equations. As

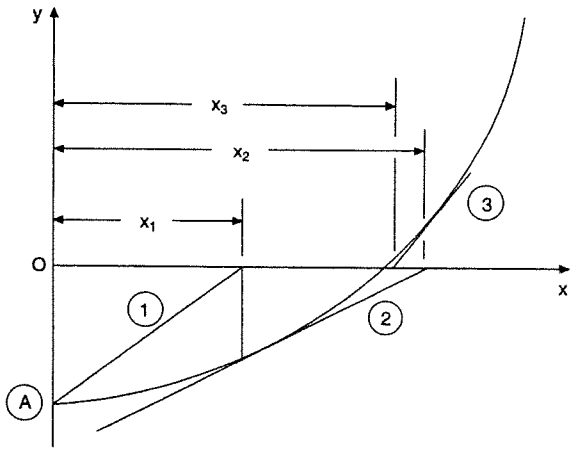

Fig. 9.5 Improved convergence in Newton Raphson method.

in the one-dimensional case the right side of these equations will not be zero for arbitrary values of $\{T\}$ and the error term which was represented as y in eq. (9.3) will now be a set of m terms. For convenience we represent the terms as $Q_1, Q_2 \ldots Q_m$ and the corresponding equations can now be represented as

$$\begin{aligned} H_{11}T_1 + H_{12}T_2 + \ldots + H_{1m}T_m - f_1 &= Q_1 \\ H_{21}T_1 + H_{22}T_2 + \ldots + H_{2m}T_m - f_2 &= Q_2 \\ \text{— — — — — — — — — — — — — —} & \\ \text{— — — — — — — — — — — — — —} & \\ H_{m1}T_1 + H_{m2}T_2 + \ldots + H_{mm}T_m - f_m &= Q_m \end{aligned} \quad \ldots (9.15)$$

or

$$[H]\{T\} - \{f\} = \{Q\} \quad \ldots (9.16)$$

As in the one-dimensional case, we represent vectors $\{Q\}$ and $\{T\}$ at the end of the n-th iteration by an upper suffix n and eqs. (9.16) and (9.15) will now be represented as

$$[H^n]\{T^n\} - \{f\} = \{Q^n\} \quad \ldots (9.17)$$

or

$$\begin{aligned} H^n_{11}T^n_1 + H^n_{12}T^n_2 + \ldots + H^n_{1m}T^n_m - f_1 &= Q^n_1 \\ \text{— — — — — — — — — — — — — —} & \\ \text{— — — — — — — — — — — — — —} & \\ H^n_{m1}T^n_1 + H^n_{m2}T^n_2 + \ldots + H^n_{mm}T^n_m - f_m &= Q^n_m \end{aligned} \quad \ldots (9.18)$$

Writing the Taylor series expansion for right side terms of eq. (9.18) after n+1-th iteration and neglecting higher order terms, we obtain

$$Q_1^{n+1} = Q_1^n + \left(\frac{\partial Q_1}{\partial T_1}\right)_{\{T\}=\{T^n\}} \Delta T_1^n + \left(\frac{\partial Q_1}{\partial T_2}\right)_{\{T\}=\{T^n\}} \Delta T_2^n + \cdots + \left(\frac{\partial Q_1}{\partial T_m}\right)_{\{T\}=\{T^n\}} \Delta T_m^n \quad \ldots (9.19)$$

plus other similar equations for $Q_2^{n+1} \ldots Q_m^{n+1}$. Writing these in matrix notations we obtain

$$\{Q^{n+1}\} = \{Q^n\} + [K_T^n]\{\Delta T^n\} \quad \ldots (9.20)$$

where matrix $[K_T^n]$ is given as

$$\left[\begin{array}{cccc} \frac{\partial Q_1}{\partial T_1} & \frac{\partial Q_1}{\partial T_2} & \cdots & \frac{\partial Q_1}{\partial T_m} \\ \frac{\partial Q_2}{\partial T_1} & \frac{\partial Q_2}{\partial T_2} & \cdots & \frac{\partial Q_2}{\partial T_m} \\ \cdot & \cdot & \cdots & \cdot \\ \cdot & \cdot & \cdots & \cdot \\ \frac{\partial Q_m}{\partial T_1} & \frac{\partial Q_m}{\partial T_2} & \cdots & \frac{\partial Q_m}{\partial T_m} \end{array}\right]_{\text{at } \{T\}=\{T^n\}}$$

$$= \frac{\partial\{Q\}}{\partial\{T\}^T} \left(\text{or } \frac{\partial\{Q\}}{\partial[T]}\right) \quad \ldots (9.21)$$

This symbolic representation of the above matrix (i.e., $\partial\{Q\}/\partial\{T\}^T$) is generally used in mathematical texts [8].

Again, using the similarity with a one-dimensional case, the n-th increment in the value of vector $\{T^n\}$ (i.e., $\{\Delta T^n\}$) will be obtained by making $\{Q^{n+1}\}$ zero in (9.20) (compare eq. 9.13) and thus

$$\{\Delta T^n\} = -[K_T^n]^{-1}\{Q^n\} \quad \ldots (9.22)$$

The matrix $[K_T^n]$ is called the tangent matrix. Its definition in eq. (9.21) implies that the tangent matrix changes with each iteration and has to be recalculated with every fresh iteration. The vector $\{T\}$ after n-th iteration is given as

$$\{T^{n+1}\} = \{T^n\} + \{\Delta T^n\} \quad \ldots (9.23)$$

Iteration is continued until the convergence criterion is met. Undoubtedly this method gives improved convergence but the algebra required in writing the tangent matrix is quite involved and this limitation has precluded it from widespread use.

9.2.5 Modified Newton-Raphson Method

The time and effort required to recalculate the tangent stiffness matrix $[K_T]$ for each iteration can be reduced by following a modified procedure. This is illustrated in Fig. 9.6. After calculating the tangent matrix for the first iteration, the modifications in vector $[T]$ (i.e., $\{\Delta T^1\}$ or Δx_1 etc. in Fig. 9.6) are calculated for a few subsequent iterations using the same tangent matrix $[K_T^1]$. After several iterations the tangent matrix is recalculated and used for a few subsequent iterations. This provides reasonably fast convergence and at the same time reduces the number of times the tangent matrix is recalculated.

9.2.6 Tangent Matrix for Heat Conduction Problem

We now attempt to write a tangent matrix for a situation involving conductive heating for which the matrix equation is given as

$$[H]\{T\} - \{f\} = 0$$

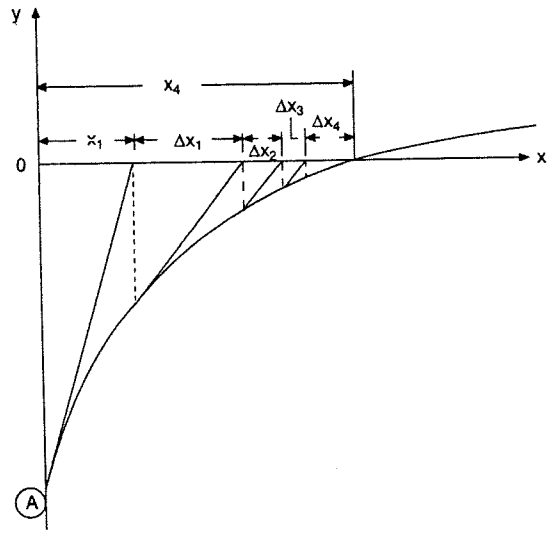

Fig. 9.6 Modified Newton Raphson method.

For temperature-dependent material properties and in situations in which the rate of internal heat generation as well as film coefficient at the convecting boundary depend on temperature, both $[H]$ and $\{f\}$ will be functions of temperature. As in the previous section, the matrix equation for temperature distribution arrived at the n-th iteration can be written as

$$\{Q^n\} = [H^n]\{T^n\} - \{f^n\} \qquad \ldots (9.24)$$

where, as explained above, vector $\{Q^n\}$ represents the residue for an arbitrary value of $\{T^n\}$, not being the final solution of the problem. The set of equations represented as (9.24) is such that each equation obtains contribution from many elements and on representing the contribution of an individual element towards i-th such equation as q_i^{ne} and f_i^{ne} we may express the i-th equation of set (9.24) as

$$Q_i^n = \sum_{e=1}^{p} q_i^{ne} - \sum_{e=1}^{p} f_i^{ne} \qquad \ldots (9.25)$$

where p represents the number of elements. If elemental $[h]$ matrix during n-th iteration is represented as $[h^{ne}]$ with its terms as h_{ij}^{ne} etc. we may write the contribution of an element to eq. (9.25) as

$$q_i^{ne} = h_{ii}^{ne} T_i^n + h_{ij}^{ne} T_j^n + \cdot + \cdot + \cdot + h_{ir}^{ne} T_r^{n(2)} \qquad \ldots (9.26)$$

where $i, j \ldots \dot{r}$ designate the nodes of an element and for a three-noded 2D triangular element the above equation becomes

$$q_i^{ne} = h_{ii}^{ne} T_i^n + h_{ij}^{ne} T_j^n + h_{ik}^{ne} T_k^n \qquad \ldots (9.27)$$

where i, j, k refer to node numbers belonging to element e. Also the individual terms h_{ij}^{ne} are given as

$$h_{ij}^{ne} = \int_{A^e} \left(k_x^n \frac{\partial N_i}{\partial x}\frac{\partial N_j}{\partial x} + k_y^n \frac{\partial N_i}{\partial y}\frac{\partial N_j}{\partial y} \right) dA \qquad \ldots (9.28)$$

k_x and k_y are thermal conductivity values in x and y direction which are the only temperature-dependent parameters here and so the current values of these at n-th iteration are k_x^n, k_y^n.

Referring back to the expression for tangent matrix (eq. 9.21) and considering the expansion of Q_i^n (in n-th iteration, eq. 9.25), we observe

[2]In this and subsequent equations in this section repetition of the suffix does not imply summation over the values of the suffix.

that various terms of i-th row of tangent matrix will be obtained by differentiating Q_i^n (eq. 9.25) with respect to individual nodal temperatures T_1, T_2 etc. Alternatively, the contribution from each element $(q_i^{ne} - f_i^{ne})$ should be differentiated with respect to nodal temperatures. From among all such possible derivatives, $\frac{\partial(q_i^{ne} - f_i^{ne})}{\partial T_1}, \frac{\partial(q_i^{ne} - f_i^{ne})}{\partial T_2}$ etc., the only three non-zero derivatives are those with respect to T_i, T_j, T_k, since elemental contributions $(q_i^{ne} - f_i^{ne})$ depend on these three nodal temperatures only. Thus the three-term contribution from element 'e' towards the terms of the i-th row of the tangent matrix (9.21) can be represented as

$$\frac{\partial q_i^{ne}}{\partial T_i} - \frac{\partial f_i^{ne}}{\partial T_i}, \frac{\partial q_i^{ne}}{\partial T_j} - \frac{\partial f_i^{ne}}{\partial T_j}, \frac{\partial q_i^{ne}}{\partial T_k} - \frac{\partial f_i^{ne}}{\partial T_k} \qquad \ldots (9.29)$$

The general term can now be expressed as follows using eqs. (9.27) and (9.28).

$$\frac{\partial q_i^{ne}}{\partial T_j} = \frac{\partial h_{ii}^{ne}}{\partial T_j} \cdot T_i^n + \frac{\partial h_{ij}^{ne}}{\partial T_j} \cdot T_j^n + \frac{\partial h_{ik}^{ne}}{\partial T_j} \cdot T_k^n + h_{ij}^{ne} \qquad \ldots (9.30)$$

Writing for $\frac{\partial}{\partial T_j}(k_x^n) = \frac{\partial k_x^n}{\partial T} \cdot \frac{\partial T}{\partial T_j} = k_x' \cdot N_j$,
we obtain the following expression after rearranging the constant terms within the integral sign

$$\frac{\partial h_{ij}^{ne}}{\partial T_j} \cdot T_j^n = \int_{A^e} \left\{ k_x' \frac{\partial N_i}{\partial x}\frac{\partial (N_j T_j^n)}{\partial x} + k_y' \frac{\partial N_i}{\partial y}\frac{\partial (N_j T_j^n)}{\partial y} \right\} N_j \, dA \qquad \ldots (9.31)$$

(Again note that repetition of suffixes does not imply summation.)
Similarly, after determining the other terms of eq. (9.30) and on combining we obtain

$$\frac{\partial q_i^{ne}}{\partial T_j} = \int_{A^e} \left\{ k_x' \frac{\partial N_i}{\partial x}\frac{\partial}{\partial x}(N_i T_i^n + N_j T_j^n + N_k T_k^n) \right\} N_j \, dA + \int_{A^e} \left\{ k_y' \frac{\partial N_i}{\partial y}\frac{\partial}{\partial y}(N_i T_i^n + N_j T_j^n + N_k T_k^n) \right\} N_j \, dA + h_{ij}^{ne}$$

$$= \int_{A^e} \left(k_x' \frac{\partial N_i}{\partial x}\frac{\partial T^n}{\partial x} + k_y' \frac{\partial N_i}{\partial y}\frac{\partial T^n}{\partial y} \right) N_j \, dA + h_{ij}^{ne} \qquad \ldots (9.32)$$

$$= h_{Dij}^{ne} + h_{ij}^{ne} \qquad \ldots (9.33)$$

Substituting in expression (9.29) and writing C_{ij}^{ne} for $\frac{\partial f_i^{ne}}{\partial T_j}$, we obtain

$$\frac{\partial q_i^{ne}}{\partial T_j} - \frac{\partial f_i^{ne}}{\partial T_j} = h_{Dij}^{ne} + h_{ij}^{ne} + C_{ij}^{ne} \qquad \text{... (9.34)}$$

The other two terms can be obtained by changing the suffixes. This element will also contribute the similar three terms in the two other rows of the tangent matrix (eq. 9.21) (i.e. j-th and k-th rows). Thus the nine-term contribution from an element towards the overall tangent matrix will be the sum of three submatrices formed by terms given in eq. (9.34). Or

$$[K_T^{ne}] = [h_D^{ne}] + [h^{ne}] - [C^{ne}] \qquad \text{... (9.35)}$$

The general terms of these matrices are given in eqs. (9.32), (9.28) and (9.34) respectively. Assembling all such elemental submatrices will yield the tangent matrix $[K_T^n]$ as

$$[K_T^n] = \sum_{e=1}^{p} [K_T^{ne}] = \sum_{e=1}^{p} [h_D^{ne}] + \sum_{e=1}^{p} [h^{ne}] - \sum_{e=1}^{p} [C^{ne}]$$

$$= [H_D^n] + [H^n] - [C^n] \qquad \text{... (9.36)}$$

Extension of these expressions to a three-dimensional situation is straightforward.

9.3 IRREVERSIBLE NON-LINEARITY (PLASTICITY)

Elastoplastic behaviour of material subjected to loading is a very important example of irreversible non-linearity. In fact the post-yield behaviour of metals as well as non-metals is highly non-linear and is influenced by a number of factors, such as loading history, strain rate, temperature and loading direction. In view of its importance many attempts have been made to model it mathematically and several theories are presented each one applicable to a few materials. An attempt is made here to present an overview of the more common type for such behaviour before discussing the finite element formulation for such cases.

9.3.1 General Elastoplastic Behaviour

It is common knowledge that the unidirectional tension test gives linear stress-strain relationship only up to yield point, beyond which the slope

of the curve changes as shown in Fig. 9.7. Also, after straining the material beyond the yield point (C) up to another point on the curve (say D), if the load is removed the unloading process follows a different path (DE) which is parallel to (OC) but is shifted by an amount given by ε_p (plastic strain or permanent set). On reloading in tension after the removal of load, the stress and strain follow the path ED with a shift in yield point to a value corresponding to the point D. Again, the slope of the curve changes beyond point D and the material starts to behave plastically. It can also be seen that if the material is loaded in compression after having undergone a plastic strain ε_p in tension, a new yield point in compression is obtained (σ_{yc} in Fig. 9.7). It may be equal to the modified yield point corresponding to point D (i.e., $|\sigma_{yc}| = |\sigma_{y2}|$) or it may be lower than this ($|\sigma_{yc}| < |\sigma_{y2}|$). This second effect is a consequence of

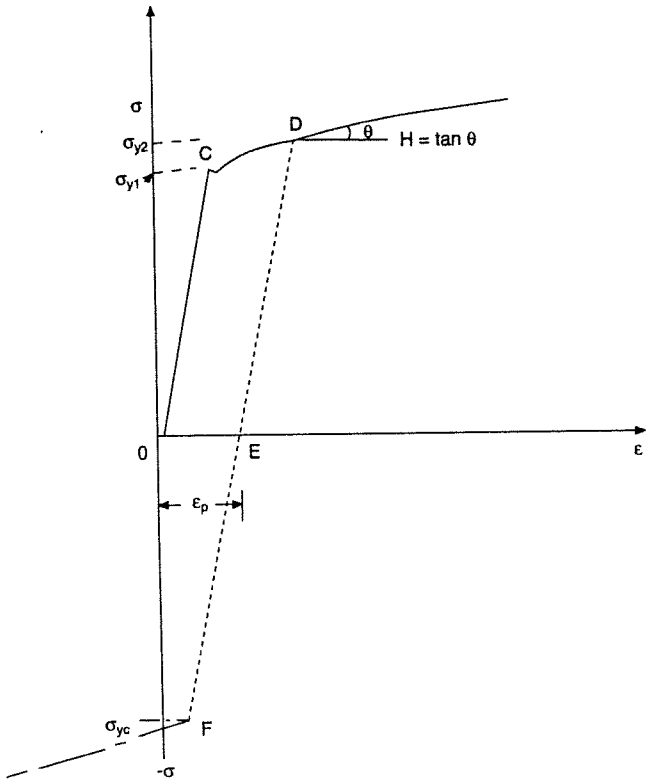

Fig. 9.7 Elasto-plastic stress-strain relation.

what is known as the Bauschinger effect. In fact, pure Bauschinger effects is the one when the sum of the magnitudes of yield points in tension and compression remain constant and is equal to $2\sigma_{y1}$ in Fig. 9.7. Thus any model of elastoplastic behaviour should be capable of reproducing these two aspects; i.e.

(1) dependence of yield point on plastic strain (strain hardening),
(2) different yield points in tension and compression after plastic straining (Bauschinger effect).

These two effects are well-known observations in the uniaxial tension test on metals and alloys. However, the real loading within a stressed body is generally multidirectional, which complicates the situation further. We shall now discuss some additional observations related to three-dimensional straining.

9.3.2 Three-dimensional Plasticity

When a body is loaded under a 3D state of stress the following additional observations are made.

(1) Yielding does not occur if the body is subjected to hydrostatic pressure from all sides, irrespective of the magnitude of the pressure. This applies to negative pressure also (i.e., tension).
(2) Common materials behave in an isotropic manner, i.e., if the same combination of stresses is applied in a different orientation, the yielding behaviour remains unaltered. This means that if normal stresses σ_1 and σ_2 are applied in x and y directions respectively, the material behaviour will not change if σ_2 is applied in x direction and σ_1 in y direction.

We shall now try to develop a mathematical model of yielding behaviour of material which is consistent with the observations presented in this section and the previous one. The model will first be developed without the Bauschinger effect and then with this effect incorporated.

Three-dimensional stress at a point has six components comprising three normal and three shear stresses. As in Chapter 2, we shall represent these as σ_x, σ_y, σ_z, τ_{xy}, τ_{yz}, τ_{zy}. It is also known that the stresses acting at a point can always be resolved into stresses along a set of three mutually perpendicular directions such that shear stresses in these directions are absent. These are called principal directions and corresponding stresses are principal stresses designated as σ_1, σ_2, σ_3. This means that any state of stress can be represented completely by the three principal stresses and associated stress directions. We may now consider a coordinate system in which the three axes represent principal axes. Such a three-dimensional principal stress space is shown in Fig. 9.8. Any point in this

coordinate space represents completely the state of stress and we shall try to find the locus of those points in this space which represent the yielding of material. The equation of such loci is called the yield criterion or yield function.

Referring to Fig. 9.8, the line OA which makes equal angles with the three axes, represents the state of pure hydrostatic pressure because the three principal stresses are equal at any point along this line. This signifies uniform compressive or tensile stress from all sides. Since hydrostatic pressure does not contribute to yielding, the stress state will reach yielding only when the deviation from this line attains some critical value. Also, since the material is isotropic and does not possess directional properties, the yield condition should reach whenever the deviation from this line approaches critical value irrespective of the direction in which such deviation is reached. Hence the yield locus should be a circle in the plane normal to OA. Also, the amount of deviation represented by yield locus remains the same irrespective of the amount of hydrostatic pressure; thus a cylinder with OA as the axis should represent the yield surface or yield condition. It can easily be seen from Fig. 9.8 that if the stress state at a point is represented by the components of vector $\vec{OD}$, then for

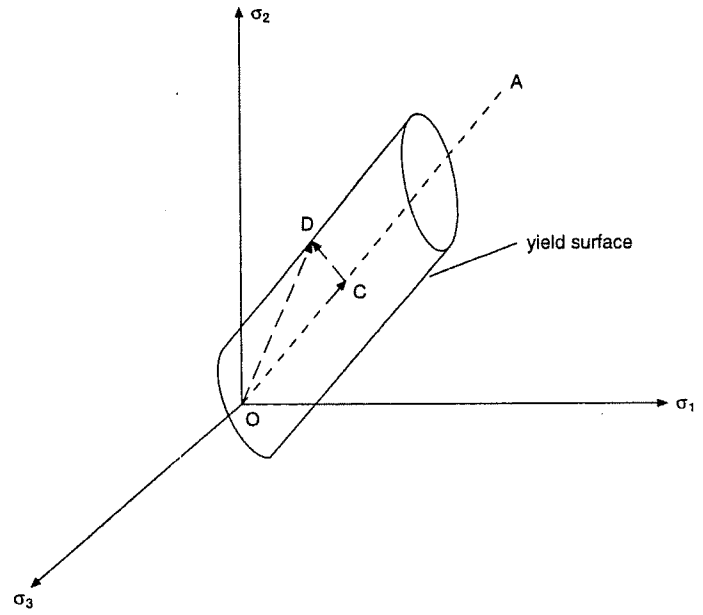

Fig. 9.8 3D yield condition in principal stress space.

yielding to occur the length of vector $\vec{CD}$ will attain a critical value irrespective of the location of point D. Also, vector $\vec{OC}$ represents pure hydrostatic state of stress and thus principal stresses at point C will be the same in all the three directions. Representing the magnitude of the component of vector $\vec{OC}$ along the direction of any principal axis by σ_{av} and considering the three principal stresses at D to be σ_1, σ_2, σ_3, we obtain the length of vector $\vec{CD}$ as

$$[(\sigma_1 - \sigma_{av})^2 + (\sigma_2 - \sigma_{av})^2 + (\sigma_3 - \sigma_{av})^2]^{1/2} = \sqrt{2}\, k \quad \text{... (9.37)}$$

where k is a constant. This equation represents the yield condition in terms of principal stresses. It can easily be shown[3] that hydrostatic stress σ_{av} is given by

$$\sigma_{av} = \frac{\sigma_1 + \sigma_2 + \sigma_3}{3} \quad \text{... (9.38)}$$

The condition given by eq. (9.37) is the well-known Von Mises' yield criterion. This equation can also be represented in various alternative forms such as

$$\left[\frac{1}{2}\{(\sigma_1 - \sigma_2)^2 + (\sigma_2 - \sigma_3)^2 + (\sigma_3 - \sigma_1)^2\}\right]^{1/2} - \sqrt{3}\, k = 0 \quad \text{... (9.39)}$$

$$\left[\frac{3}{2}\{(\sigma_x - \sigma_{av})^2 + (\sigma_y - \sigma_{av})^2 + (\sigma_z - \sigma_{av})^2 + 2(\tau_{xy}^2 + \tau_{yz}^2 + \tau_{zx}^2)\}\right]^{1/2} - \sqrt{3}\, k = 0 \quad \text{... (9.40)}$$

The parameter k can also be related to the yield strength obtained from the uniaxial tension test. In the uniaxial tension test the direction of principal stress σ_1 is the loading direction and its magnitude will be equal to yield stress, $\bar{\sigma}$. The other two principal stresses are zero. On substituting in eq. (9.39) we observe that $\bar{\sigma} = \sqrt{3}\, k$. Thus eq. (9.40) can also be written as

$$\left[\frac{3}{2}\{(\sigma_x - \sigma_{av})^2 + (\sigma_y - \sigma_{av})^2 + (\sigma_z - \sigma_{av})^2 + 2(\tau_{xy}^2 + \tau_{yz}^2 + \tau_{zx}^2)\}\right]^{1/2} - \bar{\sigma} = 0 \quad \text{... (9.40a)}$$

---

[3] $(CD)^2 = (OD)^2 - (OC)^2$

$= (\sigma_1^2 + \sigma_2^2 + \sigma_3^2) - 3\,\sigma_{av}^2$

CD is given by left-hand side of eq. (9.37) and a simplification of this will give relation (9.38)

Equation (9.40) represents yield condition in terms of six usual stress components instead of principal stresses. Equation (9.38) again gives σ_{av}, which is also equal to $(\sigma_x + \sigma_y + \sigma_z)/3$. The difference between actual stress and hydrostatic stress is also known as the deviatoric stress and these components are identified by a prime, i.e., $\sigma'_x = \sigma_x - \sigma_{av}$ etc. Since hydrostatic stress does not have shear component, $\tau'_{xy} = \tau_{xy}$ etc., eq. (9.40) is written in terms of deviatoric stresses as

$$\left[\frac{3}{2}\{\sigma_x'^2 + \sigma_y'^2 + \sigma_z'^2 + 2(\tau_{xy}'^2 + \tau_{yz}'^2 + \tau_{zx}'^2)\}\right]^{1/2} - \sqrt{3}k = 0 \quad \text{... (9.41)}$$

or $$\left[\frac{3}{2}\{\sigma_x'^2 + \sigma_y'^2 + \sigma_z'^2 + 2(\tau_{xy}'^2 + \tau_{yz}'^2 + \tau_{zx}'^2)\}\right]^{1/2} - \bar{\sigma} = 0 \quad \text{... (9.41a)}$$

Representing deviatoric stresses in tensor notations (σ'_{ij} etc.) and using the tensor summation convention (Chapter 3) expression (9.41) can be written as

$$\sqrt{\frac{1}{2}\sigma'_{ij}\,\sigma'_{ij}} - k = 0 \quad \text{... (9.42)}$$

The yield criterion is also represented symbolically as

$$F(\sigma_{ij}, k) = 0 \quad \text{... (9.43)}$$

Two-dimensional loading: The principal stress σ_3 is zero in a two-dimensional situation and the yield locus is the intersection of the cylinder shown in Fig. 9.8 with the principal plane, $\sigma_3 = 0$. This is an ellipse, as shown in Fig. 9.9. Note that there exists a hydrostatic component of stresses at every point on this ellipse whose magnitude varies from point to point along the ellipse.

9.3.3 Post-Yield Behaviour

Having established the yield criterion in three dimensions we are now

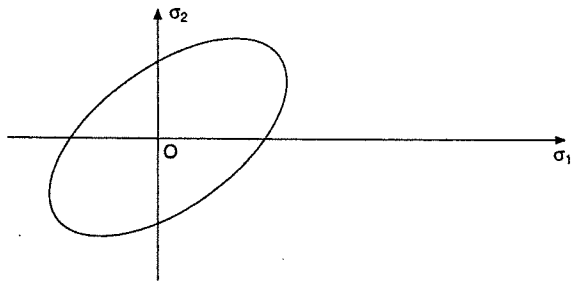

Fig. 9.9 Yield locus in 2D principal stress space.

in a position to establish post-yield behaviour, such as strain hardening, Bauschinger effect, in a 3D case. Referring to Figs. 9.8 and 9.9 as well as eq. (9.37) any increase in value of k reflects strain hardening which is equivalent to increase in radius of cylinder in Fig. 9.8 and an outward expansion of ellipse in Fig. 9.9. The strain hardening effect can thus be considered to influence only the parameter k, so k is thus dependent on the amount of plastic work done during straining. The situation corresponding to simple strain hardening in two dimensions is depicted in Fig. 9.10(a). It can be seen that the magnitude of σ_1 in uniaxial loading (i.e., $\sigma_2 = 0$) is the same be it tensile or compressive yielding. In fact, the intercept of the ellipse with σ_1 axis has increased on both sides, thus reflecting the same increase in yield point both in tension and compression. An equivalent situation in three dimensions is a uniform increase in the diameter of the cylinder; this behaviour is called *isotropic hardening*.

The Bauschinger effect is incorporated in a slightly different manner. As noted in Sec. 9.3.1 the pure Bauschinger effect is reflected by an increase in yield point in one direction (say tension) and an equal decrease in yield point in the other direction (compression). Thus the sum of the magnitudes of the two yield stresses remains fixed. This behaviour can be incorporated in a two- or three-dimensional situation by assuming a shift in position of the ellipse, as shown in Fig. 9.10(b). Note that the sum of the magnitudes of yield points in unidirection tension and compression remain constant when the ellipse shifts physically in any direction. The new centre of the ellipse is O'. The 3D case can be visualized as the physical movement of the axis of the cylinder. This type of the behaviour is called *kinematic hardening*. The symbolic representation of yield criterion (eq. 9.43) can now be

$$F\left((\sigma_{ij} - \alpha_{ij}), k\right) = 0 \qquad \ldots (9.44)$$

Here α_{ij} represent 9 components of a tensor which gives the shift of yield locus in 9-component general stress space. In 2D principal stress space it is depicted by shift of the centre of the ellipse to the new position O', as shown in Fig. 9.10(b). The magnitudes of α_{ij} are dependent on various components of plastic strains in different directions or alternatively on plastic work done during deformation. This concept can be readily incorporated in other forms of yield criterion given in Sec. 9.3.2. We can summarize the results of this discussion as follows.

The yield point in isotropic hardening is given by any of the forms of Von Mises' yield criterion stated in Sec. 9.3.2 such that the parameter k depends on the amount of plastic work performed during straining. The yield criterion in kinematic hardening, which includes the Bauschinger effect, is given by a similar form of expression where stresses $\sigma_x \cdot \sigma_y$ etc. (or σ_{ij}) are modified by a factor α_{ij}, which itself depends on the amount

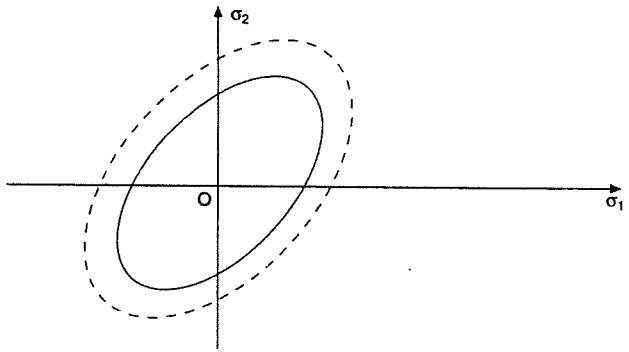

(a) Isotropic hardening

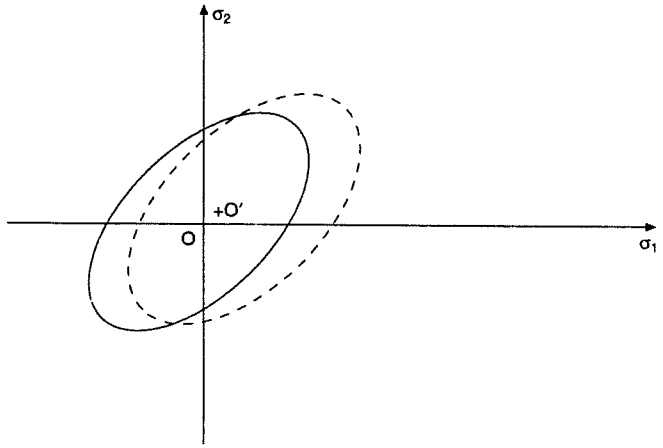

(b) Kinematic hardening

Fig. 9.10 Post-yield behaviour in two-dimensional situation.

of plastic work performed during straining. The parameter k may remain constant.

Various finite element packages, capable of elastoplastic analysis provide a choice of selecting post-yield behaviour as either isotropic hardening or kinematic hardening or a few other forms not discussed here. Another type of plastic behaviour, generally observed in hot metals and known as viscoplastic behaviour, is discussed in Chapter 10 (Sec. 10.3.1). Creep at high temperature is also an important aspect of non-linear behaviour of metals and alloys. Materials, such as rock and concrete

are modelled using the Mohr-Coulomb or Drucker-Prager yield criterion and flow rules. Complete discussion of these will be obtained in a text on plasticity [1].

Flow rule: The amount of plastic strain ε_p in a unidirectional case has a direct relationship with yield stress as represented by the stress-strain curve. The situation is not so obvious in a 3D case wherein plastic strain will also have all the normal and shear components. For elastic analysis the strain components are related to stresses by the coefficient of elasticity E and Poisson ratio ν. These relations do not apply to the plastic case. Based on some experimental observations flow rules for plastic strains were established and the well-known Prandtl-Reuss flow rule [1] is stated here.

According to the Prandtl-Reuss flow rule, the various components of incremental plastic strain are proportional to corresponding deviatoric stresses. Thus

$$d\varepsilon_{ij}^p \propto \sigma'_{ij} \qquad \ldots (9.45)$$

These represent the nine components of stress and strain tensors. When we represent this relation in terms of engineering stress, strains ε_x, ε_y, γ_{xy} etc., we get the following relation (noting that (γ_{xy} (or, γ_{12}) = $2\varepsilon_{xy}$). Thus

$$\frac{d\varepsilon_x^p}{\sigma'_x} = \frac{d\varepsilon_y^p}{\sigma'_y} = \frac{d\varepsilon_z^p}{\sigma'_z} = \frac{d\gamma_{xy}^p}{2\tau'_{xy}} = \frac{d\gamma_{yz}^p}{2\tau'_{yz}} = \frac{d\gamma_{zx}^p}{2\tau'_{zx}} = \text{constant} \quad \ldots (9.46)$$

Denoting the yield criterion given in eq. (9.40a) as 'F', we can also deduce the following relations:

$$\frac{\partial F}{\partial \sigma_x} = \frac{3\sigma'^{(4)}_x}{2\bar{\sigma}}; \frac{\partial F}{\partial \sigma_y} = \frac{3\sigma'_y}{2\bar{\sigma}}; \frac{\partial F}{\partial \sigma_z} = \frac{3\sigma'_z}{2\bar{\sigma}};$$

[4] Writing F in terms of σ_x, σ_y, σ_z, τ_{xy}, τ_{yz}, τ_{zx} and substituting $\bar{\sigma}$ for $\sqrt{3}\,k$ in eq. (9.40a), we obtain

$$F \equiv \left[\frac{3}{2}\left\{\left(\frac{2\sigma_x}{3} - \frac{\sigma_y}{3} - \frac{\sigma_z}{3}\right)^2 + \left(\frac{2\sigma_y}{3} - \frac{\sigma_x}{3} - \frac{\sigma_z}{3}\right)^2 + \left(\frac{2\sigma_z}{3} - \frac{\sigma_x}{3} - \frac{\sigma_y}{3}\right)^2 + 2(\tau_{xy}^2 + \tau_{yz}^2 + \tau_{zx}^2)\right\}\right]^{1/2} - \bar{\sigma} = 0.$$

Differentiating F with respect to σ_x

$$\frac{\partial F}{\partial \sigma_x} = \frac{1}{2\bar{\sigma}}\left[2\left(\frac{2\sigma_x}{3} - \frac{\sigma_y}{3} - \frac{\sigma_z}{3}\right) - \left(\frac{2\sigma_y}{3} - \frac{\sigma_x}{3} - \frac{\sigma_z}{3}\right) - \left(\frac{2\sigma_z}{3} - \frac{\sigma_x}{3} - \frac{\sigma_y}{3}\right)\right]$$

Now substituting $\sigma_{av} = (\sigma_x + \sigma_y + \sigma_z)/3$ and $\sigma'_x = \sigma_x - \sigma_{av}$,

$$\frac{\partial F}{\partial \sigma_x} = \frac{3\sigma'_x}{2\bar{\sigma}}$$

$$\frac{\partial F}{\partial \tau_{xy}} = \frac{3\tau'_{xy}}{\bar{\sigma}}; \frac{\partial F}{\partial \tau_{yz}} = \frac{3\tau'_{yz}}{\bar{\sigma}}; \frac{\partial F}{\partial \tau_{zx}} = \frac{3\tau'_{zx}}{\bar{\sigma}}; \qquad \ldots (9.47)$$

On substituting these in eq. (9.46) we can also express the flow rule as

$$d\varepsilon_x^p = \frac{2\bar{\sigma}}{3}\frac{\partial F}{\partial \sigma_x}(C); d\varepsilon_y^p = \frac{2\bar{\sigma}}{3}\frac{\partial F}{\partial \sigma_y}(C);$$

$$d\gamma_{xy}^p = \frac{2\bar{\sigma}}{3}\frac{\partial F}{\partial \tau_{xy}}(C) \text{ etc.} \qquad \ldots (9.48)$$

Here (C) is the constant of proportionality. Denoting incremental plastic strains and the quantities represented in expression (9.47) by the following vectors

$$\{d\varepsilon^p\}^T = [d\varepsilon_x^p, d\varepsilon_y^p, d\varepsilon_z^p, d\gamma_{xy}^p, d\gamma_{yz}^p, d\gamma_{zx}^p] \qquad \ldots (9.49)$$

$$\left\{\frac{\partial F}{\partial \sigma}\right\}^T = \left[\frac{3}{2\bar{\sigma}}\sigma'_x, \frac{3}{2\bar{\sigma}}\sigma'_y, \frac{3}{2\bar{\sigma}}\sigma'_z, \frac{3}{\bar{\sigma}}\tau'_{xy}, \frac{3}{\bar{\sigma}}\tau'_{yz}, \frac{3}{\bar{\sigma}}\tau'_{zx}\right], \qquad \ldots (9.50)$$

we can write the flow rule in a more compact form in terms of engineering stress strains as

$$\{d\varepsilon^p\} = \left\{\frac{\partial F}{\partial \sigma}\right\} d\lambda, \qquad \ldots (9.51)$$

where $d\lambda$ is equal to the constant (C) of eq. (9.46) multiplied by $2\bar{\sigma}/3$. Sometimes instead of using yield criterion "F" in eq. (9.51) another function of stresses, called plastic potential, Q, is used and $\{\partial F/\partial\sigma\}$ is replaced by $\{\partial Q/\partial\sigma\}$. However, for most materials Q is taken to be the same as F and we shall consider this case only. Further details of plastic potential and its behaviour can be obtained from a standard text on plasticity [1]. The type of plastic behaviour when $Q \equiv F$ is also known as associated plasticity.

9.3.4 Approach to Finite Element Analysis

Usual discretization of the domain will precede finite element analysis. Loading has to be incremental and in small steps so that after every load step the elements can be checked for plastic yielding or otherwise. Thus we need to obtain an incremental stress-strain relation of the form

$$\{d\sigma\} = [D_{ep}]\{d\varepsilon\} \qquad \ldots (9.52)$$

Here $[D_{ep}]$ is some sort of elastoplastic matrix. We now proceed to

develop that relation. The vector representing increment in total strain $\{d\varepsilon\}$ will consist of two components; elastic strain increments and plastic strain increments. The elastic strain increments will be related to incremental stress through elasticity matrix [D] (Chapter 2). Thus we write

$$\{d\varepsilon\} = \{d\varepsilon^e\} + \{d\varepsilon^p\}$$

$$= [D]^{-1}\{d\sigma\} + \left\{\frac{\partial F}{\partial \sigma}\right\} d\lambda \qquad \ldots (9.53)$$

The unknown coefficient $d\lambda$ is determined by utilizing the concept of plastic work and the results of uniaxial stress-strain curve. Plastic work is defined as[5]

$$dw = \sigma'_x\, d\varepsilon^p_x + \sigma'_y\, d\varepsilon^p_y + \ldots + \tau'_{zx}\, d\gamma^p_{zx}$$

$$= \{\sigma'\}^T\{d\varepsilon^p\} = \{\sigma'\}^T\left\{\frac{\partial F}{\partial \sigma}\right\} d\lambda = \bar{\sigma}\cdot d\lambda \qquad \ldots (9.54)$$

Only deviatoric stress components have been considered here because hydrostatic components of stress do not contribute to yielding. We also make use of the yield criterion (9.41a) written in symbolic form as

$$F(\sigma_x, \sigma_y \ldots, \bar{\sigma}) = 0 \qquad \ldots (9.55)$$

Here k is replaced by uniaxial yield stress $\bar{\sigma}$ and the tensorial stress components of eq. (9.43) are replaced by corresponding engineering stress components. The yield stress $\bar{\sigma}$ is a function of plastic work dw and thus the seven independent parameters of eq. (9.55) are σ_x, σ_y, ... τ_{zx} and dw. Since the right side of the equation is always zero, the Taylor series expansion of F gives us

$$dF = \frac{\partial F}{\partial \sigma_x} d\sigma_x + \frac{\partial F}{\partial \sigma_y} d\sigma_y + \frac{\partial F}{\partial \sigma_z} d\sigma_z + \frac{\partial F}{\partial \tau_{xy}} d\tau_{xy} +$$

$$+ \frac{\partial F}{\partial \tau_{yz}} d\tau_{yz} + \frac{\partial F}{\partial \tau_{zx}} d\tau_{zx} + \frac{\partial F}{\partial w} dw = 0$$

[5] Logically speaking, the incremental plastic work should be given by the sum of the products of total stresses and incremental plastic strains, i.e.,

$$dw = \sigma_x\, d\varepsilon^p_x + \sigma_y\, d\varepsilon^p_y + \ldots \tau_{zx}\, d\gamma^p_{zx}$$

Since $\sigma_x = \sigma'_x + \sigma_{av}$ etc. and $\tau'_{zx} = \tau_{zx}$,
hence

$$dw = \sigma'_x\, d\varepsilon^p_x + \sigma'_y\, d\varepsilon^p_y + \ldots \tau'_{zx}\, d\gamma^p_{zx} + \sigma_{av}\,(d\varepsilon^p_x + d\varepsilon^p_y + d\varepsilon^p_z).$$

The term within parentheses represents volumetric plastic strain and there being no volume change during plastic strain, the volumetric plastic strain is zero.

or

$$\left\{\frac{\partial F}{\partial \sigma}\right\}^T \{d\sigma\} + \frac{\partial F}{\partial w} dw = 0 \qquad \ldots (9.56)$$

Replacing dw by eq. (9.54):

$$\left\{\frac{\partial F}{\partial \sigma}\right\}^T \{d\sigma\} + \frac{\partial F}{\partial w}\bar{\sigma}\cdot d\lambda = 0 \qquad \ldots (9.57)$$

Results of the uniaxial tension test can be used to determine $(\partial F/\partial w)$. We know from Fig. 9.7 that the plastic work during strain increment $d\varepsilon_p$ is $dw = \sigma\, d\varepsilon_p$, being the area under the curve. Here σ is the yield stress at the point under consideration. It is shown in Sec. 9.3.5 that σ is same as equivalent stress $(\bar{\sigma})$ in case of uniaxial tension test. If slope of stress-plastic strain curve is H, then on replacing σ by $\bar{\sigma}$

$$d\bar{\sigma} = H\, d\varepsilon_p \qquad \ldots (9.57a)$$

Thus,

$$dw = \bar{\sigma}\cdot\frac{1}{H} d\bar{\sigma}$$

or,

$$\frac{d\bar{\sigma}}{dw} = \frac{H}{\bar{\sigma}}$$

Again, taking F to be represented by eq. (9.41a) we obtain $(\partial F/\partial w)$ as

$$\frac{\partial F}{\partial w} = \frac{\partial F}{\partial \bar{\sigma}}\cdot\frac{d\bar{\sigma}}{dw} = -\frac{H}{\bar{\sigma}} \qquad \ldots (9.58)$$

Substituting in (9.57),

$$\left\{\frac{\partial F}{\partial \sigma}\right\}^T \{d\sigma\} - H\, d\lambda = 0 \qquad \ldots (9.59)$$

$d\lambda$ can be eliminated from eqs. (9.53) and (9.59). Observing that H is indeterminate for perfectly plastic material care should be taken neither to divide nor to multiply eqs. (9.53) or (9.59) by H. Multiplying (9.53) by $\left\{\frac{\partial F}{\partial \sigma}\right\}^T [D]$ and subtracting (9.59) from it, we get

$$\left\{\frac{\partial F}{\partial \sigma}\right\}^T [D]\{d\varepsilon\} = \left\{\frac{\partial F}{\partial \sigma}\right\}^T [D]\left\{\frac{\partial F}{\partial \sigma}\right\} d\lambda + H d\lambda$$

or $$\left\{\frac{\partial F}{\partial \sigma}\right\}^T [D]\{d\varepsilon\} = (3G + H)\, d\lambda^{(6)} \quad \ldots (9.60)$$

Here G is shear modulus. Substituting $d\lambda$ from (9.60) into eq. (9.53)

$$\{d\varepsilon\} = [D]^{-1}\{d\sigma\} + \left\{\frac{\partial F}{\partial \sigma}\right\}\left\{\frac{\partial F}{\partial \sigma}\right\}^T [D]\{d\varepsilon\} \cdot \frac{1}{(3G + H)}$$

or $$\left[[D] - [D]\left\{\frac{\partial F}{\partial \sigma}\right\}\left\{\frac{\partial F}{\partial \sigma}\right\}^T [D] \cdot \frac{1}{(3\,G + H)}\right]\{d\varepsilon\} = \{d\sigma\} \quad \ldots (9.61)$$

The elastoplastic matrix $[D_{ep}]$ (of eq. 9.52) is given by the quantity within brackets in eq. (9.61). It can be simplified further if we observe from footnote[6] that

$$\left\{\frac{\partial F}{\partial \sigma}\right\}^T [D] = \frac{3G}{\bar{\sigma}}[\sigma'_x\ \sigma'_y\ \sigma'_z\ \tau'_{xy}\ \tau'_{yz}\ \tau'_{zx}]$$

---

[6]Partition $\left\{\frac{\partial F}{\partial \sigma}\right\}$ and $[D]$ as

$$\left\{\frac{\partial F}{\partial \sigma}\right\} = \begin{Bmatrix} F_1 \\ F_2 \end{Bmatrix};\ [D] = \begin{bmatrix} D_{11} & 0 \\ 0 & D_{22} \end{bmatrix}$$

where

$$\{F_1\} = \frac{3}{2\bar{\sigma}}\begin{Bmatrix} \sigma'_x \\ \sigma'_y \\ \sigma'_z \end{Bmatrix};\ \{F_2\} = \frac{3}{\bar{\sigma}}\begin{Bmatrix} \tau'_{xy} \\ \tau'_{yz} \\ \tau'_{zx} \end{Bmatrix};$$

$$[D_{11}] = A\begin{bmatrix} 1 & \frac{\nu}{(1-\nu)} & \frac{\nu}{(1-\nu)} \\ \frac{\nu}{(1-\nu)} & 1 & \frac{\nu}{(1-\nu)} \\ \frac{\nu}{(1-\nu)} & \frac{\nu}{(1-\nu)} & 1 \end{bmatrix};\ [D_{22}] = A\frac{(1-2\nu)}{2(1-\nu)}\begin{bmatrix} 1 & 0 & 0 \\ 0 & 1 & 0 \\ 0 & 0 & 1 \end{bmatrix};$$

we thus obtain

$$\left\{\frac{\partial F}{\partial \sigma}\right\}^T [D]\left\{\frac{\partial F}{\partial \sigma}\right\} = \{F_1\}^T [D_{11}]\{F_1\} + \{F_2\}^T [D_{22}]\{F_2\} = \frac{3}{2}\frac{E}{(1+\nu)} = 3\,G.$$

Here

$$A = \frac{E(1-\nu)}{((1+\nu)(1-2\nu))}$$

and $$[D]\left\{\frac{\partial F}{\partial \sigma}\right\} = \left[\left\{\frac{\partial F}{\partial \sigma}\right\}^T [D]\right]^T$$

Matrix $[D_{ep}]$ of eq. (9.61) can now be expressed as $[D_{ep}] = [D] - [D_p]$ such that

$$^{(7)}[D_p] = \frac{(3G)^2}{\bar{\sigma}^2\,(3G + H)} \times$$

$$\begin{bmatrix} \sigma'^2_x & \sigma'_x\sigma'_y & \sigma'_x\sigma'_z & \sigma'_x\tau'_{xy} & \sigma'_x\tau'_{yz} & \sigma'_x\tau'_{zx} \\ & \sigma'^2_y & \sigma'_y\sigma'_z & \sigma'_y\tau'_{xy} & \sigma'_y\tau'_{yz} & \sigma'_y\tau'_{zx} \\ & & \sigma'^2_z & \sigma'_z\tau'_{xy} & \sigma'_z\tau'_{yz} & \sigma'_z\tau'_{zx} \\ & & & \tau'^2_{xy} & \tau'_{xy}\tau'_{yz} & \tau'_{xy}\tau'_{zx} \\ & & & & \tau'^2_{yz} & \tau'_{yz}\tau'_{zx} \\ & & & & & \tau'^2_{zx} \end{bmatrix} \quad \ldots (9.62)$$

The solution procedure will now involve use of large load step(s) in the beginning using simple elastic analysis until the stress in any element reaches (or exceeds) the yield criterion. From this stage onwards small load steps should be used following the incremental relation given by eq. (9.52). The actual procedure is explained in the next section.

9.3.5 Another Method of Presenting Experimental Stress-Plastic Strain Relation

The stress-strain relation is traditionally presented from the results of a uniaxial tension test in the form of a curve with uniaxial stress and strain as the two axes (Fig. 9.7). The actual stress state at a point in a body being three-dimensional, it has six components of stress and strain.

---

[7]H used in eq. (9.62) is the local slope of effective stress-effective plastic strain curve or for the uniaxial test it is the slope of stress vs plastic strain curve. Some researchers [3, 4] prefer the use of second slope of the stress-strain curve, E_T shown in Fig. 9.11. The relation between H, E and E_T can now be developed. If incremental stress and strain, $d\sigma$ and $d\varepsilon$ are considered, $d\varepsilon$ will be made of elastic and plastic parts. Thus

$$d\varepsilon = d\varepsilon_e + d\varepsilon_p = \frac{d\sigma}{E} + d\varepsilon_p$$

Since $d\varepsilon = d\sigma/E_T$ and $d\varepsilon_p = d\sigma/H$ (H being slope of stress-plastic strain curve while E_T is slope of stress-total strain curve), on substitution, we obtain

$$\frac{d\sigma}{E_T} = \frac{d\sigma}{E} + \frac{d\sigma}{H} \quad \therefore H = \frac{EE_T}{E - E_T}.$$

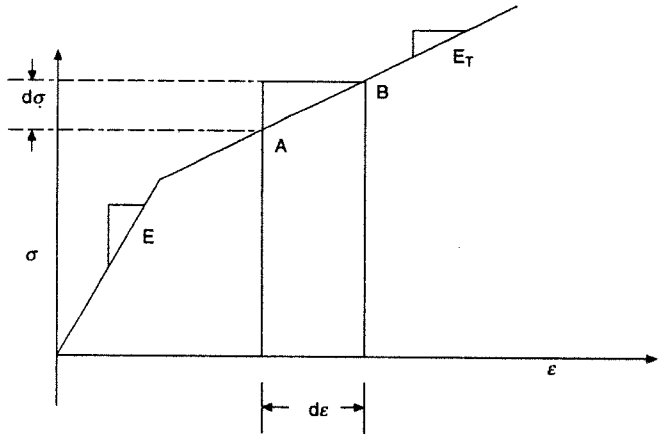

Fig. 9.11

In order to make a correlation between actual stress state and the results of a uniaxial tension test feasible, the curve is interpreted in terms of effective stress, $\bar{\sigma}$, and effective plastic strain, $\bar{\varepsilon}$, defined as follows:

$$\bar{\sigma} = \left[\frac{3}{2}\{\sigma_x'^2 + \sigma_y'^2 + \sigma_z'^2 + 2(\tau_{xy}'^2 + \tau_{yz}'^2 + \tau_{zx}'^2)\}\right]^2 \quad \ldots (9.63)$$

(see eq. 9.41a)

$$\bar{\varepsilon} = \left[\frac{2}{3}\left\{\varepsilon_x^{p2} + \varepsilon_y^{p2} + \varepsilon_z^{p2} + \frac{1}{2}(\gamma_{xy}^{p2} + \gamma_{yz}^{p2} + \gamma_{zx}^{p2})\right\}\right]^{1/2[8]} \quad \ldots (9.64)$$

It is interesting to observe that the magnitudes of effective stress and effective plastic strain for the uniaxial tension test are equal to direct stress and plastic strain[9] (axial stress and plastic strain along specimen axis). Hence the simple stress vs plastic strain curve can be interpreted as effective stress-effective plastic strain curve and in this form it can be used for three-dimensional stress analysis. Also, if it is possible to devise

[8]There being no volume change during plastic straining ($\varepsilon_x^p + \varepsilon_y^p + \varepsilon_z^p = 0$ for small strains), the total as well as deviatoric components of plastic strains are equal.

[9]From volume consistency condition and due to symmetry of tensile test specimen, the plastic strains ε_y^p and ε_z^p will both be equal to $-\varepsilon_x^p/2$. Shearing strains being absent we find, on substitution, that $\bar{\varepsilon} = \varepsilon_x^p$. .Similarly, total stress being σ_x in x-direction and zero in y and z directions ($\sigma_y = \sigma_z = 0$), the hydrostatic component will be $\sigma_x/3$ and the deviatoric stresses will be $\sigma_x' = 2\sigma_x/3$, $\sigma_y' = -\sigma_x/3$, $\sigma_z' = -\sigma_x/3$. On substitution in eq. (9.63), we obtain $\bar{\sigma} = \sigma_x$.

a test in which the specimen is loaded under a multiaxial stress system [13] then effective stress and strain would provide a very convenient means of presenting the experimental relationship.

9.3.6 Incremental Elastoplastic Stress-Strain Analysis

The procedure for elastoplastic stress analysis can now be summarized. It involves the following steps.

1) Apply the loads in increments involving several load steps. The first load step can be large enough but only to the extent that all the elements remain within the elastic limit. The displacement calculations will be based on the relation

$$[K]\{\delta\} - \{F\} = 0 \quad \ldots (9.65)$$

where $[K]$ is the stiffness matrix obtained on assembling the elemental stiffness matrices $[K^e]$ defined as

$$[K^e] = \int_{V^e} [B]^T [D][B]\, dV \quad \ldots (9.66)$$

and

$$[K] = \sum_{e=1}^{n} [K^e] \quad \ldots (9.66a)$$

This follows the procedure of Chapter 2 where $[D]$ is the elastic stress-strain matrix. Equation (9.65) can also be interpreted as

$$[K]\{\Delta\delta^1\} - \{\Delta F^1\} = 0 \quad \ldots (9.67)$$

where $\{\Delta\delta^1\}$ and $\{\Delta F^1\}$ represent the incremental displacement and load in the first load step in which loading is fully elastic.

2) Apply the second increment in load $\{\Delta F^2\}$ and first use elastic analysis to obtain nodal displacements and stresses. Determine the effective stress and compare it with yield stress. Then determine the elements in which plastic yielding has occurred in this load step (effective stress > yield stress). Proceed to step 3.
3) For the current increment in load $\{\Delta F^n\}$ the incremental nodal displacements are determined using elastoplastic analysis by applying the following relation,

$$[K]\{\Delta\,\delta^n\} - \{\Delta\, F^n\} = 0 \quad \ldots (9.68)$$

Stiffness matrix $[K]$ is again obtained as the vector sum of elemental stiffness matrices $[K^e]$ by using eq. (9.66a). Matrix $[K^e]$ is obtained by using eq. (9.66) if the element is loaded within elastic limits even after application of load in the current load step (which may be determined when iterations are performed within the

load step). If plastic loading occurs, matrix $[K^e]$ is obtained by the relation

$$[K^e] = \int_{V^e} [B]^T [D_{ep}] [B] \, dV^{(10)} \qquad \ldots (9.69)$$

4) The incremental stress (elastic or elastoplastic) is determined again in all the elements by using the incremental displacements $\{\Delta\delta^n\}$ calculated in step 3 (say by using eq. 9.52). The state of stress is updated by adding incremental stress to the state of stress of the previous *load step*. Then effective stress is determined which is compared with the yield stress prevailing in the element. Iterations within the current load step are repeated (step 3 above) if either of the following two conditions are present:
   (i) If any element has changed its status from elastic to elastoplastic or vice versa.
   (ii) Even if an element continues to remain in a plastic state, if the magnitude of effective stress in it differs substantially from the yield stress there, this means converged plastic strain has not been attained.

   Strategies adopted to satisfy condition (ii) above are discussed in the next section. Only when all the convergence criteria (stated above) have been met can we proceed to the next load step by repeating 3-4 for additional load increments.
5) Finally, when all the load steps have been completed, we determine the total plastic strain, stress etc. in various elements.

Several strategies have been proposed for updating the stresses and plastic strains as mentioned in step 3 or for checking the convergence stated in step 4. Since elastoplastic analysis involves use of many small load increments with a number of iterations within each load step, these strategies are aimed at reducing this computational effort while obtaining the accuracy desired in the solution. In one approach [6, 7], the size of load increment is chosen in a manner that only one additional element enters into plastic range within a load step. If this criterion is violated the load step is reduced to satisfy it. In general, these procedures involve use of a large number of load increments with the elastoplastic matrix updated in each load increment.

[10]This is based on the incremental relation

$$[K]\{\Delta\delta\} - \{\Delta F\} = 0.$$

Such an incremental load displacement relation is obtained by using the principle of minimization of complementary energy [5] which applies to elastic as well as plastic loading or elastic unloading.

9.3.7 Iterative Elastoplastic Analysis and Initial Stress Method

Iterative procedures are based on the approach similar to Newton-Raphson approach in which the tangent matrix is used to update the nodal displacement vector in successive iteration. Early attempts, such as initial stress or initial strain approaches in which the elasticity matrix was used for formulating the tangent stiffness matrix and non-linearity was considered through use of an adjustable load vector term $\{f_{\sigma 0}\}$ were not very successful due to the high degree of non-linearity existing in elastoplastic analysis. However, later modifications in the form of mixed incremental-cum-iterative procedure which considered loads in incremental steps (step size being larger compared to pure incremental technique (Sec. 9.3.6) with the tangent stiffness matrix based on elastoplastic relations gave improved results and better convergence. These methods have now found favour with investigators and several ingenious procedures have been developed.

The foundation of such methods was laid in the 1960s by Zienkiewicz and coworkers [2]. Minimization of potential energy was chosen as the basis. Thus equating the incremental potential energy to zero, we obtain

$$\Delta\Pi = \sum_{e=1}^{n} \int_{V^e} \{d\varepsilon\}^T \{\sigma\} \, dV - \{\Delta\delta\}^T \{F\} = 0 \qquad \ldots (9.70)$$

We can replace $[d\varepsilon]$ by $\{B\}\{\Delta d^e\}$ which is true by the definition of strains (Chapter 2). The stress $\{\sigma\}$ is now a non-linear function of strain and available only in the incremental form for the elastoplastic case (eq. 9.61). Since the direct relationship between $\{\sigma\}$ and $\{\varepsilon\}$ is not available we retain $\{\sigma\}$ as such in eq. (9.70) and thus obtain

$$\Delta\Pi = \sum_{e=1}^{n} \{\Delta d^e\}^T \int_{V^e} [B]^T \{\sigma\} \, dV - \{\Delta\delta\}^T \{F\} = 0 \qquad \ldots (9.71)$$

The assembly operation performed on the first term of eq. (9.71) gives

$$\{\Delta\delta\}^T \left\{ \sum_{e=1}^{n} \int_{V^e} [B]^T \{\sigma\} \, dV \right\} - {}^{(11)}\{\Delta\delta\}^T \{F\} = 0 \qquad \ldots (9.72)$$

or

$$\{\Delta\delta\}^T \{Q\} = 0$$

where $\{Q\}$ is a vector of the same order as $\{\Delta\delta\}$ and is given by

[11]Considering a triangular element, it can be seen that the quantity $\int_{V^e} [B]^T \{\sigma\} \, dV$ is a 6×1 vector which is multiplied by a 1×6 vector $\{\Delta d^e\}^T$. When such contributions are assembled from all elements, the overall sum can be written as the product of incremental nodal displacement vector $\{\Delta\delta\}^T$ and a vector of the same order as $\{\Delta\delta\}$ shown as vector summation of contributions from all elements.

$$\{Q\} = \sum_{e=1}^{n} \int_{V^e} [B]^T \{\sigma\}\, dV - \{F\} \qquad \ldots (9.73)$$

Since the expression for incremental potential energy is valid for any small displacement vector $\{\Delta\delta\}$ with components of arbitrary magnitude, the only way in which eq. (9.72) can be satisfied is that all the components of vector $\{Q\}$ be zero[12]. Hence eq. (9.73), equated to zero, gives the non-linear equation to be solved. After expressing $\{\sigma\}$ in terms of nodal displacement, this equation can be solved to obtain the displacements and stresses etc. The solution should now be obtained by using the Newton-Raphson method in which vector $\{Q\}$ can be treated as residue for any arbitrary displacement $\{\delta\}$. This residue is to be brought to zero after successive iterations, as explained in Sec. 9.2.3. The relation for m-th iteration will be similar to eq. (9.22), i.e.

$$\{\Delta\delta^m\} = -[K_T^m]^{-1} \{Q^m\} \qquad \ldots (9.74)$$

where $\{\Delta\delta^m\}$ is the improvement in the value of $\{\delta\}$ as obtained in the m-th iteration and $[K_T^m]$ is the tangent-stiffness matrix in the m-th iteration obtained by replacing T by δ in eq. (9.21). Symbolically the tangent matrix (eq. 9.21) is written as $\dfrac{\partial\{Q\}}{\partial\{\delta\}^T}\left(\text{or } \dfrac{\partial\{Q\}}{\partial[\delta]}\right)$[13]

Differentiating $\{Q\}$ from eq. (9.73) with respect to $\{\delta\}$ and recognizing $\{F\}$ as constant, we obtain

$$[K_T] = \frac{\partial\{Q\}}{\partial\{\delta\}^T} = \sum_{e=1}^{n} \int_{V^e} [B]^T \frac{\partial\{\sigma\}}{\partial\{\varepsilon\}^T} \frac{\partial\{\varepsilon\}}{\partial\{d^e\}}\, dV \qquad \ldots (9.75)$$

In this expression we made use of the fact that stresses in an element are functions of elemental strains only, which per se are functions of elemental nodal displacement. The term $\dfrac{\partial\{\sigma\}}{\partial\{\varepsilon\}^T}$ is obtained from eqs. (9.52) and (9.62) as $[D_{ep}]$ for elements undergoing plastic deformation and $[D]$ for other elements not undergoing plastic deformation (see *Exer. 9.1*). Substituting $[B]\{d^e\}$ for $\{\varepsilon\}$ we also obtain

[12] $\{\Delta\delta\}^T \{Q\} = \Delta\delta_1 Q_1 + \Delta\delta_2 Q_2 + \ldots = 0$. Since $\Delta\delta_1, \Delta\delta_2 \ldots$ are arbitrary, hence $Q_1 = 0$, $Q_2 = 0, \ldots$

[13] Such relations and corresponding matrices are given in [8]. In particular, when $\{Q\}$ is a function of another vector (say $\{A\}$) and $\{A\}$ itself is a function of $\{C\}$, the following relation holds good.

$$\frac{\partial\{Q\}}{\partial\{C\}^T} = \frac{\partial\{Q\}}{\partial\{A\}^T} \cdot \frac{\partial\{A\}}{\partial\{C\}^T}$$

This can also be verified by writing these matrices in expanded form and then multiplying them. It will yield the usual relation of partial differentation. See also *Exer. 9.1.*

$$\frac{\partial\{\varepsilon\}}{\partial\{d^e\}} = [B]$$

Thus eq. (9.75) becomes

$$[K_T] = \sum_{e=1}^{n} \int_{V^e} [B]^T [D_{ep}] [B]\, dV \qquad \ldots (9.76)$$

We note that $[D_{ep}]$ is replaced by $[D]$ for those elements which are not subjected to plastic loading.

The difference between the initial stress method and the mixed incremental-cum-iterative method is that the former uses elasticity matrix $[D]$ throughout to determine tangent stiffness matrix $[K_T^n]$ which does not differ from $[K]$. During successive improvements in the values of displacement $\{\Delta\delta^n\}$, the plastic strains are considered in the form of modification in load vector $\{\Delta F_{in}\}$ shown in Fig. 9.12a. The latter method uses different tangent stiffness matrices within different load increments. This is determined on the basis of the elemental elastoplastic matrix $[D_{ep}]$ at the beginning of the particular load increment. The situation is schematized in Fig. 9.12b. These methods are further detailed in the following discussion.

Exercise 9.1: Vectors $\{X\}$ and $\{t\}$ are n component vectors defined as

$$\{X\}^T = [x_1, x_2, \ldots x_n];\ \{t\}^T = [t_1, t_2, \ldots t_n]$$

and each $x_1, x_2, x_3 \ldots x_n$ can be expressed as functions of $t_1, t_2 \ldots t_n$. Also the incremental vectors $\{dX\}$ and $\{dt\}$ are related through the matrix $[C]$ as

$$\{dX\} = [C]\ \{dt\}$$

where $[C]$ is an $n \times n$ matrix. Show that matrices $[C]$ and $\dfrac{\{\partial X\}}{\{\partial t\}^T}$ are identical.

Hint: Use simple partial differentiation of $x_1, x_2 \ldots x_n$ to obtain components of matrix $[C]$. It will be observed that these are same as the components of matrix $\dfrac{\{\partial X\}}{\{\partial t\}^T}$.

a) Initial stress method [2]: This method proceeds as follows. We load the structure and first obtain an elastic solution by substituting $\{\sigma\} = [D][B]\{d^e\}$ in eq. (9.73) and taking the left side as zero. The equation will have the form

$$[K]\ \{\delta\} - \{F\} = 0 \qquad \ldots (9.77)$$

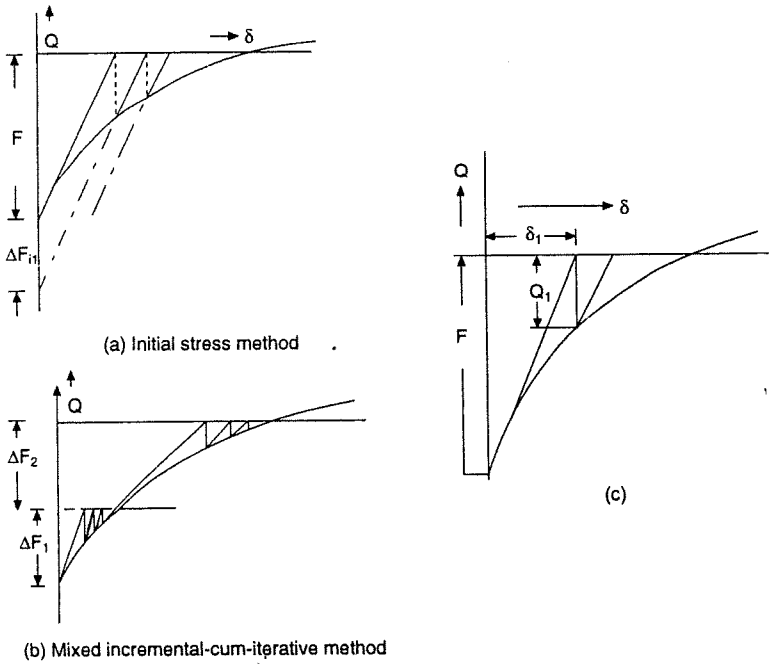

Fig. 9.12 Various alternative approaches of elastoplastic analysis.

The first trial solution of nodal displacements $\{\delta^1\}$ can be obtained from this equation. Elastic strains and stresses in the elements are obtained as $\{\varepsilon_1^e\}$ and $\{\sigma_1^e\}$ where suffix 1 refers to first trial solution (iteration). If the load is large the stresses in some of the elements may exceed the yield criterion and in order to satisfy the yield condition these stresses have to be brought down to a level consistent with the flow rule. Several situations may arise. If we symbolically represent the yield criterion as $F(\{\sigma\}, k) = 0$ and if the loading started from an initially unstressed state we may have either $F(\{\sigma_1^e\}, k) < 0$, a purely elastic case in which no modification is required, or $F(\{\sigma_1^e\}, k) > 0$ which means the material has yielded. In the latter case we determine the equivalent strain $\bar{\varepsilon}$ corresponding to trial elastic strain $\{\varepsilon_1^e\}$ and bring it to yield point (say by proportional reduction). Designating this modified strain as $\{\varepsilon_1^e\}_m$ we obtain the difference between $\{\varepsilon_1^e\}$ and $\{\varepsilon_1^e\}_m$ as inelastic strain designated as $\{\Delta\varepsilon_1^e\}_{in}$. Thus

$$\{\Delta\varepsilon_1^e\}_{in} = \{\varepsilon_1^e\} - \{\varepsilon_1^e\}_m \qquad \ldots (9.78)$$

Also the stress in this element is taken to be yield stress corresponding to strain $\{\varepsilon_1^e\}_m$ and its magnitude is represented as $\{\sigma_1^e\}_m$. The incremental stress in the element is now determined by using the elastoplastic relation (eq. 9.52). The inelastic strain $\{\Delta\varepsilon_1^e\}_{in}$, determined above, is taken as the incremental strain. Thus

$$\{\Delta\sigma_1^e\} = [D_{ep}]\{\Delta\varepsilon_1^e\}_{in} \qquad \ldots (9.79)$$

The net stress in the element is now the sum of this stress increment and the initial stress at the start of yielding or at the beginning of load increment, whichever be the case. (If the element had yielded in the previous load increment, then the stress at the beginning of the current increment will be yield stress.) Thus we obtain net stress as

$$\{\sigma_2^e\} = \{\sigma_1^e\}_m + \{\Delta\sigma_1^e\} \qquad \ldots (9.80)$$

where $\{\sigma_2^e\}$ is the elemental stress at the beginning of the second iteration. This state of stress, which represents the true state of stress at the end of the first iteration, is different from initial trial stress $\{\sigma_1^e\}$, which itself was determined by solving eq. (9.73) with $\{Q\} = 0$. However $\{\sigma_2^e\}$ may not be the final solution and substitution of this value of stress in eq. (9.73) will yield some residue as $\{Q_1\}$. Representing the Newton-Raphson approach schematically in Fig. 9.12c, this residue is represented as Q_1 for one variable case. This $\{Q_1\}$ can be used in eq. (9.74) to obtain $\{\Delta\delta_1\}$. Note that $[K_T]$ is determined from eq. (9.75) or (9.76). Use of stress $\{\sigma_2^e\}$ in eq. (9.73) for calculating $\{Q_1\}$ in each iteration appears somewhat cumbersome and it is interesting to consider an alternative approach suggested in Ref. [2]. This approach is as follows.

Since $\{\sigma_1^e\}_m$ is the stress at the start of yielding under current load (increment) (or the stress at the start of load increment if the material was within plastic range at the start), then the difference between the trial elastic stress calculated above, $\{\sigma_1^e\}$, and yield stress after current load increment $\{\sigma_2^e\}$ (eq. 9.80) gives the amount of some unaccounted stress which results in the residue $\{Q_1\}$ in eq. (9.73). In Ref. [2] this stress is called initial stress $\{\Delta\sigma_i\}$ or

$$\{\Delta\sigma_i\} = \{\sigma_1^e\} - \{\sigma_2^e\} \qquad \ldots (9.81)$$

The Newton-Raphson approach (Fig. 9.12(c)) shows that substitution of stress which exists at the end of current iteration (i.e. $\{\sigma_2^e\}$) into eq. (9.73) should yield a residue $\{Q_1\}$, i.e.

$$\{Q_1\} = \sum_{e=1}^{n} \int_{V^e} [B]^T \{\sigma_2^e\}\, dV - \{F\} \qquad \ldots (9.82)$$

Substituting from eq. (9.81), we obtain

$$\{Q_1\} = \sum_{e=1}^{n} \int_{V^e} [B]^T \{\sigma_1^e\}\, dV - \sum_{e=1}^{r} \int_{V^e} [B]^T \{\Delta\sigma_i^e\}\, dV - \{F\} \quad \ldots (9.83)$$

Summation in the second term on the right side is done over r elements only, which represent the number of elements in which yielding has occurred. We also observe that $\{\sigma_1^e\}$ was obtained in step 1 above by solving eq. (9.73) with $\{Q\} = 0$. Hence eq. (9.83) reduces to

$$\{Q_1\} = -\sum_{e=1}^{r} \int_{V^e} [B]^T \{\Delta\sigma_i^e\}\, dV = -\{F_{i1}\} \quad \ldots (9.84)$$

The vector $\{\Delta F_{i1}\}$ which takes care of unaccounted stress (or initial stress) $\{\Delta\sigma_i\}$ now replaces $\{Q_1\}$ and can be added to vector $\{F\}$, thus giving eq. (9.73) as

$$\sum_{e=1}^{n} \int_{V^e} [B]^T \{\sigma\}\, dV - \{F\} - \{\Delta F_{i1}\} = 0 \quad \ldots (9.85)$$

Iterations are now continued by solving eq. (9.85) for trial stress $\{\sigma_k^e\}$ (say, in k-th iteration) which are modified to satisfy yield criterion as explained above. The correction load vector $\{\Delta F_{ik}\}$ is determined and added to load vector of eq. (9.85). The procedure is continued until correction vector $\{\Delta F_{ik}\}$ reduces to an insignificant amount.

It is reported that convergence is generally achieved in 3-4 iterations [2].

b) Summary of initial stress approach: The procedure discussed above can be summarized in the following steps.

(1) Apply initial load and use elastic analysis to determine trial displacement, strain and stress as $\{\delta_1\}$, $\{\varepsilon_1^e\}$ and $\{\sigma_1^e\}$ respectively.
(2) Apply yield criterion and determine whether the effective stress in any element exceeds the current yield stress.
(3) For the element which shows yielding, bring down the trial stress and strain to the value corresponding to the yield surface prevailing at the start of the iterative step (say by proportional reduction). This strain and stress can be designated as modified strain $\{\varepsilon_1^e\}_m$ and modified stress $\{\sigma_1^e\}_m$[14].
(4) Calculate the difference between trial strain and modified strain which gives the magnitude of inelastic strain as

[14]If the element was already in the plastic stage at the start of the current iterative step, the stress at that condition is supposed to be at the yield surface. A check is necessary, however, because the use of relation (9.79) may have resulted in some departure from yield surface.

$$\{\Delta\varepsilon_1^e\}_{in} = \{\varepsilon_1^e\} - \{\varepsilon_1^e\}_m$$

(5) The actual stress increment corresponding to this inelastic strain can now be determined using the elastoplastic stress-strain relation for the elements which have yielded. Thus

$$\{\Delta\sigma_1^e\} = [D_{ep}]\{\Delta\varepsilon_1^e\}_{in}$$

(6) Add stress increment $\{\Delta\sigma_1^e\}$ to the modified stress $\{\sigma_1^e\}_m$ calculated in step 3 to determine the stress at the end of current iteration which is $\{\sigma_2^e\}$ for the first iteration. This is the stress at the start of the next iteration.
(7) The difference between trial stress $\{\sigma_1^e\}$ and the stress calculated in step 6 remains unaccounted now. Zienkiewicz et al. [2] account for it as initial stress.
(8) Substituting the stress value at the end of current iteration $\{\sigma_2^e\}$ in eq. (9.73) we get the residue $\{Q\}$ to be used in the Newton-Raphson approach. Instead of calculating $\{Q\}$ an alternative approach is proposed in Ref. [2] and, as shown in the preceding section, this interpretation results in the presence of a load vector $\{\Delta F_i\}$ which takes care of unbalance (residue) in eq. (9.73). This vector is given by eq. (9.84). The equation to be solved now becomes

$$\sum_{e=1}^{n} \int_{V^e} [B]^T \{\sigma\}\, dV - \{F\} - \{\Delta F_i\} = 0$$

(9) Thus with corrected load vector $\{F\} + \{\Delta F_i\}$ we recalculate trial elastic strain and stress, and determine the corresponding modification in the load vector, $\{\Delta F_i\}$ using steps 1–8 explained above. The procedure is continued until the subsequent correction in the load vector becomes sufficiently small to be neglected. The stress and strain after this iteration now become the final quantities at the end of present load.

A major computational advantage of this method is that vector $\{\Delta F_i\}$ is to be determined only for those elements which have gone into plastic range. Also, the first term of eq. (9.85) which yields $[K]\{\delta\}$ always uses the stiffness matrix $[K]$ determined on the basis of elasticity matrix $[D]$, thus avoiding recomputation in every iteration. The procedure is somewhat similar to the modified Newton-Raphson approach in which the tangent matrix is not changed during several iterations (Fig. 9.12(c)). Q_1 shown in the Figure may be visualized as force correction vector ΔF_{i1} in Fig. 9.12a.

c) Geometrical interpretation of stress correction: The procedure of stress modification used in the preceding sections can also be visualized through geometrical representation in the principal stress and strain space. For illustration we consider a two-dimensional situation where the yield surfaces (loci) in principal stress and strain spaces are shown in Fig. 9.13. (also see Fig. 9.9).

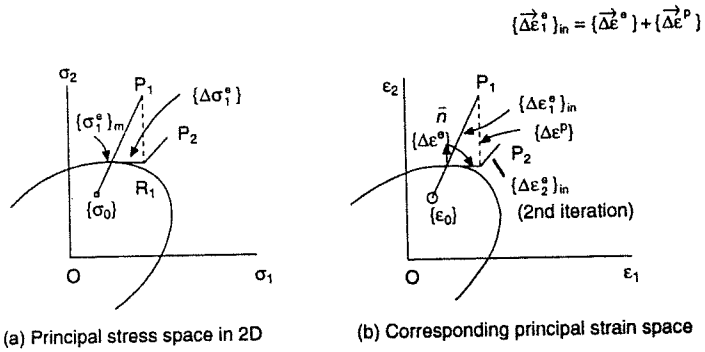

(a) Principal stress space in 2D

$$\{\vec{\Delta\varepsilon}_1^e\}_{in} = \{\vec{\Delta\varepsilon}^e\} + \{\vec{\Delta\varepsilon}^p\}$$

(b) Corresponding principal strain space

Fig. 9.13 Geometric interpretation fo stress correction.

We start with initial stress $\{\sigma_0\}$ and strain $\{\varepsilon_0\}$. These will be zero if the loading starts from an unstressed state. The corresponding points will then be located at the origin in both principal stress and strain spaces. Note that the yield locus is similar in both principal stress and strain spaces. On loading and considering elastic deformation only, the stress and strain states are represented by point P_1 in respective spaces. The inelastic incremental strain $\{\Delta\varepsilon_1^e\}_{in}$, mentioned in the preceding section, is assumed to be the total strain and will have elastic and plastic components $\{\Delta\varepsilon^e\}$ and $\{\Delta\varepsilon^p\}$ as shown in Fig. 9.13(b). This is consistent with the Prandtl-Reuss flow rule that the plastic strains are normal to yield surface. The elastic strain component $\{\Delta\varepsilon^e\}$ provides a means of calculating the stress increment $\{\Delta\sigma_1^e\}$. However, we already have a relation between total strain increment $\{\Delta\varepsilon_1^e\}_{in}$ and the stress increment $\{\Delta\sigma_1^e\}$ in the form of an elastoplastic stress-strain relation (eq. 9.52); using this we determine stress increment directly. Next the load correction vector $\{\Delta F_i\}$ is determined and a fresh loading point is obtained with this modified load. This point is shown as P_2 in Fig. 9.13. The process thus continues until the load correction vector becomes negligible.

9.3.8 Radial Return Method

Krieg and Krieg [9] presented the theoretical basis of a method known as the radial return method for determining the state of stress in an iterative step of elastoplastic analysis, shown by point R_1 in Fig. 9.13(a). This method, it is claimed, has been in use in a computer code since 1964. The unique feature of the method is that it does not require the use of elastoplastic matrix $[D_{ep}]$ to determine stress increment in step 5 of the previous section (9.3.7(b)). Thus the calculations are considerably simplified. In order to understand the method, we again use the geometrical representation of yield surface but instead of using the principal stress space, we draw the yield surface in principal deviatoric stress space. Referring to Sec. 9.3.2 and Fig. 9.8, the yield surface in principal stress space is represented by a cylinder for non-hardening plasticity. The axis of the cylinder represents hydrostatic state of stress and since hydrostatic stress has no influence on plastic flow the cylinder is assumed to extend up to infinity on both sides of origin. Now if we consider the yield criterion given by eq. (9.40) and express it in terms of principal deviatoric stresses by taking shear stress as zero in these directions, we obtain

$$\left[\frac{3}{2}\{\sigma_1'^2 + \sigma_2'^2 + \sigma_3'^2\}\right]^{1/2} - \sqrt{3}\,k = 0 \qquad \ldots (9.86)$$

This is the equation of a sphere in principal deviatoric stress space. Hence the yield criterion is represented by the surface of a sphere around the origin, irrespective of the magnitude of hydrostatic stress. This is shown in Fig. 9.14. The method explained in the preceding section is again presented in Fig. 9.14(a). For convenience it is called the tangent stiffness method because it relies on the use of tangent matrix $[D_{ep}]$ for the calculation of stress increment $\{\Delta\sigma_1^e\}$. On bringing the hypothetical loading point P_1 (trial state) back to yield surface, the total stress increment can be visualized as distance BR_1 in the Figure. The radial return method is shown at (b) in this Figure. Here the state of stress at the end of the first iteration is obtained directly by drawing the stress vector at point P_1 as $\vec{OP}_1$. The intersection of this vector with the yield surface gives the new stress state R_1. The load correction vector $\{\Delta F_i\}$ is again calculated and a new trial stress state (point P_2) is determined. The second stress state R_2 is again determined using radial return procedure and iterations continued until the incremental load correction vector $\{\Delta F_i\}$ becomes negligible. It is easy to visualize that the two procedures will result in converged solutions not far from each other. In fact, calculations performed by Krieg and Krieg [9] show that the error with respect to the exact solution is nearly the same in both the cases. The method of determining the new stress state represented by point R_1 (Fig. 9.14b) is straightforward. The stress at P_1 is given as $\{\sigma_1^e\}$. Since the two vectors $\vec{OP}$ and $\vec{OR}_1$

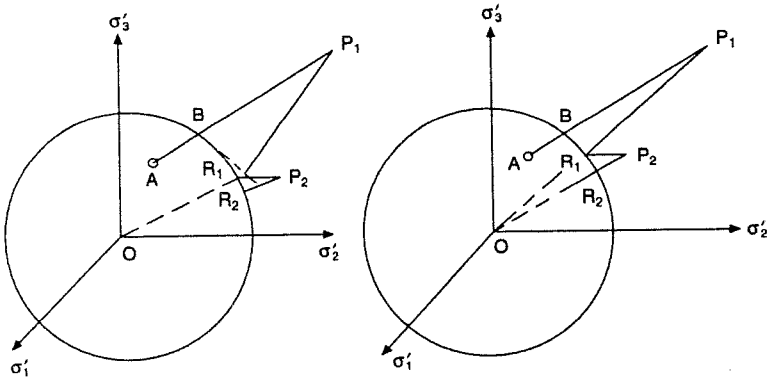

(a) Tangent stiffness method (Section 9.3.7c)

(b) Radial return method

Fig. 9.14 Tangent stiffness and radial return methods in 3D deviatoric principal stress space.

are collinear, the components of these will be proportional to each other. Also, the length of vector $\vec{OR}_1$ is obtained from the equation of sphere (eq. 9.86) as $\sqrt{2}\,k\left(\text{or } \sqrt{\frac{2}{3}}\cdot\bar{\sigma}\right)$. Similarly, length of vector $\vec{OP}_1$ is given by

$$S = \{\sigma_x'^2 + \sigma_y'^2 + \sigma_z'^2 + 2(\tau_{xy}^2 + \tau_{yz}^2 + \tau_{zx}^2)\}^{1/2} \qquad \ldots (9.87)$$

Hence the components of vector $\vec{OR}$ are obtained simply by proportional reduction (compare with eq. 9.80) as

$$\{\sigma_2^e\} = \sqrt{\frac{2}{3}}\,\frac{\bar{\sigma}}{S}\,\{\sigma_1^e\} \qquad \ldots (9.88)$$

It is the simplicity of eq. (9.88) which makes the method very attractive. The reduced amount of computation required in this method has made it popular with users.

Comparison of the two methods: Simplicity of calculations is the main advantage of the radial return method over the tangent stiffness method. Another method proposed by Rice and Tracy [10], called the secant stiffness method, offers no special advantage and is not discussed here. Between the two methods discussed above, although the radial return method offers computational advantage, it should be recognized that the tangent stiffness matrix, $[D_{ep}]$ in eq. (9.79), is calculated only for those elements which undergo plastic yielding. This calculation is replaced by eq. (9.88) in the radial return method. If there are only a few elements

which undergo plastic deformation, computational advantage is only marginal. However, for complex configuration with many elements undergoing elastoplastic straining, the advantage may be substantial.

9.3.9 Mixed Incremental and Iterative Approach

The iterative method discussed in the preceding section does not always result in the convergence to the correct solution. The reason is the dependence of this method on trial elastic solution, which may follow a path very different form the real path followed by elastoplastic deformation. When a complex loading pattern or high degree of stress concentration is present, it is essential that the load be applied in several incremental steps so that the complex path followed by actual loading is captured properly. The present trend is to use a mixed approach in which loading is incremental and analysis within an incremental load step is iterative. The load steps are obviously larger than those used in the pure incremental approach. Such a mixed method has been used by Bushnell [3], Simo and Taylor [11] and others. The main feature of these approaches is that analysis for each load step is independent except that it uses the stresses present at the beginning of load increment as initial stress and the plastic state of an element as well as the yield stress in it is adopted from the previous load step and preserved in the current step. Additionally, the elastoplastic tangent stiffness matrix is determined from the stress state existing at the start of increment by using appropriate elastoplastic matrix $[D_{ep}]$ and this replaces the purely elastic stiffness matrix used in the procedure explained in the previous section. Details of its theoretical foundation were given in Sec. 9.3.6. This stiffness matrix, however, does not change during iterations within the load step. The method thus appears somewhat similar to the modified Newton-Raphson method and improves the accuracy as well as convergence compared to the pure iterative method.

9.3.10 Conclusion: Elastoplastic Analysis

Two main approaches to elastoplastic analysis are:

(i) Pure incremental approach,
(ii) Mixed incremental-cum-iterative approach.

The pure incremental approach follows the natural process of elastoplastic deformation. It uses very small load increments and the elastoplastic matrix consistent with the plastic state prevalent during this incremental load step is used to calculate incremental displacement and stresses. For sufficiently small load steps convergence with always be achieved and the correct solution obtained. The only drawback of

this method is the large amount of computation involved in determining the elastoplastic matrix for each incremental load step.

The iterative approach which uses the elastic stiffness matrix throughout computations and accommodates the effect of plastic flow by considering a corrective load vector based on the so-called initial stress concept is an innovation which reduces computational effort drastically. There is no other logic for using this method and it fails to converge when a complex elastoplastic loading path is used.

The middle path of using the incremental-cum-iterative approach has been quite successful; the elastic predictor and plastic corrector type of approach, used in tangent stiffness and radial return methods, are just mathematical simplifications. It is obvious that the actual state of stress in the material will never follow a path which envisages an initial rise of stress to a very high value and subsequent drop to a value consistent with the yield surface. However, the justification for this oversimplification lies in its capability in predicting the actual state of stress to reasonable accuracy [9]. The major reduction in computational effort associated with this approach is the main factor behind its popularity.

Yet the pure incremental approach has merits if the computational efforts could be reduced. In the author's opinion this method has been left out in the middle of development and large reduction in computational effort could be obtained were a method devised whereby only the elemental stiffness matrix for the elements undergoing plastic deformation needs to be changed, instead of changing the complete stiffness matrix for the whole domain during each incremental step.

9.4 ILLUSTRATIVE EXAMPLES

Elastoplastic analysis forms an important application of non-linear analysis. The following example illustrates how it is used in the design of a reducer for a high-pressure pipeline [12]. A reducer used for connecting a large pipe to a smaller diameter pipe was studied. The bore diameters at the two ends were 200 and 300 mm. The thickness at the small end was 8 mm while that at the large end was 10 mm, consistent with the corresponding pipe diameters. The nominal design pressure was 4 MPa. Axi-symmetric analysis was performed and although the element configuration was not reported, a large number of elements have to be used, as reported in analysis of a similar part (Fig. 9.15(b)). Growth of the plastic zone at pressure much above the design pressure was studied on the basis of finite element analysis and the same is reported in Fig. 9.15(a) for different pressures in the range 11.2 – 22.0 MPa. The plastic zone started from the bend at the smaller end and grew as the pressure increased. Finally, an experimental burst test was

performed and the reducer burst at the location shown in Fig. 9.15(c) at a pressure of 28 MPa. As can be seen from the Figure, the location of the burst is consistent with the growth of the plastic zone and the burst occurred at the region of maximum plastic flow obtained on the basis of numerical analysis.

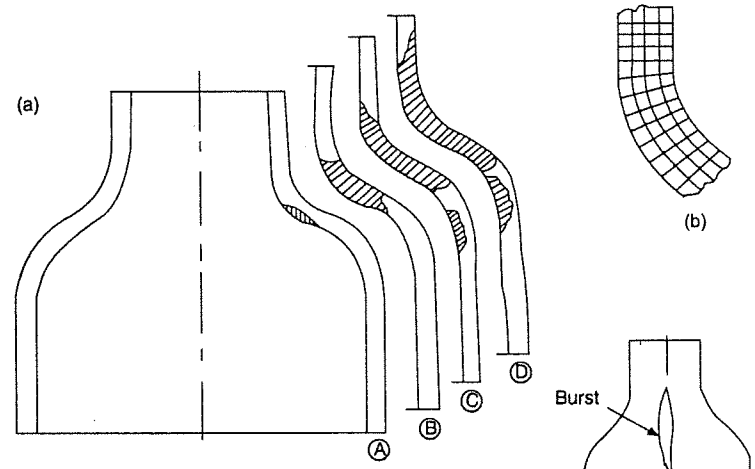

Fig.	Pressure
A	11.2 MPa
B	15.0
C	18.8
D	22.0

(a) Growth of plastic zone
(b) Mesh used
(c) Location of burst during hydraulic test

Fig. 9.15 Plastic zone in concentric pipe reducer.

REFERENCES

1. Chen, W.F. and Han, D.J. (1988). *Plasticity for Structural Engineers*. Springer-Verlag.
2. Zienkiewicz, O.C., Valliappan, S. and King, I.P. (1969). Elastoplastic solutions of engineering problems. Initial stress, finite element approach. *Int. J. Num. Meth. Engg.*, 1: 75–100.
3. Bushnell, D. (1977). A strategy for the solution of problems involving large deflections, plasticity and creep. *Int. J. Num. Meth. Engg.*, 11: 683–708.
4. Bathe, K.J. (1982). *Finite Element Procedures in Engineering Analysis*. Prentice-Hall, Englewood Cliffs, N.J.
5. Seely, F.B. and Smith, J.O. (1952). *Advanced Mechanics of Materials*. John Wiley and Sons, N.Y.
6. Biswas, K. and Gupta, O.P. (1980). Fracture mechanics evaluation of implant test. *Proc. Nat. Welding Seminar-'80*. Indian Institute of Welding, Calcutta, paper 19, pp. 1–9.
7. Biswas, K. (1991). An Investigation into the Application of J-Integral Approach to Implant Weldability Test Specimen. Ph.D. thesis, IIT, Kharagpur.
8. Norrie, D.H. and DeVries, G. (1978). *An Introduction to Finite Element Analysis*. Academic Press, N.Y.